

UNCLASSIFIED

SECURITY CLASSIFICATION OF THIS PAGE (When Data Entered)

REPORT DOCUMENTATION PAGE		READ INSTRUCTIONS BEFORE COMPLETING FORM
1. REPORT NUMBER ENVPREDRSCHFAC Technical Note No. 21	2. GOVT ACCESSION NO.	3. RECIPIENT'S CATALOG NUMBER
4. TITLE (and Subtitle) NVA Upper Air Temperature and Wind Analysis for a 12-Level European Area Model		5. TYPE OF REPORT & PERIOD COVERED
		6. PERFORMING ORG. REPORT NUMBER
7. AUTHOR(s) A. Groll		8. CONTRACT OR GRANT NUMBER(s)
9. PERFORMING ORGANIZATION NAME AND ADDRESS Environmental Prediction Research Facility Naval Postgraduate School Monterey, CA 93940		10. PROGRAM ELEMENT, PROJECT, TASK AREA & WORK UNIT NUMBERS PE: 62759N PN: 52551 TA: WF52-551-713 EPRE WU: 054:2-2
11. CONTROLLING OFFICE NAME AND ADDRESS Naval Air Systems Command Department of the Navy Washington, D.C. 20360		12. REPORT DATE June 1975
		13. NUMBER OF PAGES 53
14. MONITORING AGENCY NAME & ADDRESS (if different from Controlling Office)		15. SECURITY CLASS. (of this report) UNCLASSIFIED
		15a. DECLASSIFICATION/DOWNGRADING SCHEDULE
16. DISTRIBUTION STATEMENT (of this Report) Approved for public release; distribution unlimited.		
17. DISTRIBUTION STATEMENT (of the abstract entered in Block 20, if different from Report)		
18. SUPPLEMENTARY NOTES		
19. KEY WORDS (Continue on reverse side if necessary and identify by block number) Numerical variational analysis (NVA) Euler's equation of motion 12-level non-staggered model Upper-air temperature and wind analysis		
20. ABSTRACT (Continue on reverse side if necessary and identify by block number) A numerical variational upper-air temperature and wind analysis (NVA) is developed for a 12-level non-staggered half-mesh grid for the European-Mediterranean area. The goal is to establish a computational concept and efficient relaxation method for solving the fourth order non-linear set of partial difference equations encountered in NVA by applying Euler's equation of motion to an atmosphere assumed to be in hydrostatic equilibrium.		

UNCLASSIFIED

20. Abstract (continued)

The behavior of convergence of the system's equations toward a stable solution was investigated with respect to arbitrarily chosen weights on the initial data fields.

To demonstrate the effect of random noise in the initial fields, a random generator was applied to the input and the power spectra of input and output were determined.

No effort was made to evaluate the usefulness of the different systems' solutions from a synoptic point of view because it was felt that data fields most apt to initialize a forecast model need not be the best representatives of the actual states of the atmosphere. However, different solutions are presented for differently chosen weights.

AN (1) AD-A013 192
FG (2) 040200
CI (3) (U)
CA (5) ENVIRONMENTAL PREDICTION RESEARCH FACILITY (NAVY)
MONTEREY CALIF
TI (6) NVA Upper Air Temperature and Wind Analysis for a
12-Level European Area Model.
TC (8) (U)
DN (9) Technical note,
AU (10) Groll, A.
RD (11) Jun 1975
PG (12) 53p
RS (14) ENVPREDRSCHF-tech note-21
PJ (16) WF52-551
TN (17) WF52-551-713
RC (20) Unclassified report
DE (23) *Weather forecasting, Wind, Atmospheric temperature,
Partial differential equations, Equations of motion,
Numerical integration, Atmosphere models, Europe
DC (24) (U)
ID (25) Variational methods, Numerical weather forecasting
IC (26) (U)
AB (27) A numerical variational upper-air temperature and wind
analysis (NVA) is developed for a 12-level
non-staggered half-mesh grid for the
European-Mediterranean area. The goal is to establish a
computational concept and efficient relaxation method
for solving the fourth order non-linear set of partial
difference equations encountered in NVA by applying
Euler's equation of motion to an atmosphere assumed to
be in hydrostatic equilibrium.
AC (28) (U)
DL (33) 01
CC (35) 407279

FOREWORD

This document is based on the mathematical research published in the Technical Report for Task 4 of Contract No. N66314-73-C-1591 for the Environmental Prediction Research Facility, Monterey, California, prepared by Philip G. Kesel and Howard L. Lewit.

The finite difference equations are expanded to a 12-level non-staggered model. To achieve more rapid convergence and to be more economical with respect to computer storage, the relaxation method was changed to sequential relaxation across vertical planes of the grid. Stable solutions were reached within 800 sec on the Control Data Corporation (CDC) 6500 computer in most cases.

Approved for public release.
Distribution unlimited

LIBRARY
TECHNICAL REPORT SECTION
NAVAL POSTGRADUATE SCHOOL
MONTEREY, CALIFORNIA 93940

ENVPREDRSCHFAC
Technical Note No.-21

NVA UPPER AIR TEMPERATURE AND
WIND ANALYSIS FOR A 12-LEVEL
EUROPEAN AREA MODEL

by

A. Groll

June 1975

// Environmental Prediction Research Facility
Naval Postgraduate School
Monterey, California 93940

Qualified requestors may obtain additional copies from the Defense Documentation Center. All others should apply to the National Technical Information Service.

CONTENTS

FOREWORD	1
1. INTRODUCTION	5
2. APPLICATION OF THE NUMERICAL VARIATIONAL ANALYSIS METHOD	6
2.1 DYNAMICAL CONSTRAINT	7
2.2 VARIATIONAL TECHNIQUE AND ASSOCIATED EULER EQUATIONS	8
2.3 FINITE DIFFERENCING SCHEME AND RELAXATION TECHNIQUE	9
3. SOLUTIONS	12
3.1 CONVERGENCE OF THE FINITE DIFFERENCE APPROXIMATION	12
3.2 CONVERGENCE TOWARD STABLE SOLUTIONS WITH RESPECT TO ARBITRARILY CHOSEN WEIGHTS	16
3.3 DISCUSSION OF DIFFERENT SOLUTIONS DERIVED FROM DIFFERENT SETS OF WEIGHTS	18
4. SOME ASPECTS OF THE SPECTRAL ANALYSIS OF INITIAL GUESS AND NVA FIELDS	45
5. CONCLUSIONS	51
REFERENCES	53

1. INTRODUCTION

Initialization of a forecast model does not necessarily mean analyzing meteorological data at given grid points in order to give a representation of the actual state of the atmosphere as accurately as possible. It mainly means analyzing the data in such a way that the prognostic equations of the forecast model can cope without producing spurious gravity waves due to the fact that the initial analysis is not in balance with the physical constraint impressed on the atmosphere by a given set of prognostic equations.

Although these waves are eventually suppressed to reasonable magnitudes during the time-iterating process -- due to geostrophic adjustment, for example, in PE models -- the problem remains for short range forecasts up to 24 hours.

This report describes a computational concept for initializing a 12-level PE window model for the European-Mediterranean area. Upper-air temperature and wind analyses are performed, utilizing the Numerical Variational Analysis (NVA) technique.

2. APPLICATION OF THE NUMERICAL VARIATIONAL ANALYSIS METHOD

The goal of the following upper-air temperature and wind analyses is to minimize the mean square deviation between the measured quantities \tilde{T} , \tilde{u} , and \tilde{v} and the finally analyzed quantities T , u , and v over a 3-dimensional domain of the atmosphere. Thus the functional

$$J_* = \int \int \int_S [(u-\tilde{u})^2 + (v-\tilde{v})^2 + (T-\tilde{T})^2] dx dy dz \quad (1)$$

must be minimized.

The assumption that the atmosphere is in hydrostatic equilibrium and follows Euler's equation of motion, and that the equation of state can be accomplished, leads to auxiliary conditions in T , u , and v which are introduced into (1) as a weak constraint (see Sasaki, 1970a) giving

$$J = \int \int \int_S [\alpha(u-\tilde{u})^2 + \alpha(v-\tilde{v})^2 + \beta(T-\tilde{T})^2 + \gamma F^2 + \gamma G^2] dx dy dz \quad (2)$$

and its first variation

$$\delta J = \int \int \int_S [\alpha(u-\tilde{u})\delta u + \alpha(v-\tilde{v})\delta v + \beta(T-\tilde{T})\delta T + \gamma F\delta F + \gamma G\delta G] dx dy dz. \quad (3)$$

A priori α , β and γ are arbitrary weights determining the degree to which a term of the sum in (2) can be approximated by zero relative to the others; F and G provide the dynamical constraint and are functions of T , u , and v .

2.1 DYNAMICAL CONSTRAINT

The dynamical constraints used in this case are derived from Euler's equation of motion. Using the hydrostatic approximation, the equations are written:

$$\frac{\partial u}{\partial t} + w \cdot \nabla u - fv + \frac{\partial \phi}{\partial x} = 0 \quad (4)$$

$$\frac{\partial v}{\partial t} + w \cdot \nabla v + fu + \frac{\partial \phi}{\partial y} = 0 \quad (5)$$

$$\frac{1}{\rho} \frac{\partial p}{\partial z} + g = 0. \quad (6)$$

Introducing the vertical coordinate $\sigma = \ln\left(\frac{p_0}{p}\right)$ and the equation of state into (6), one gets

$$\frac{\partial \phi}{\partial \sigma} = \frac{p}{\rho} = RT. \quad (7)$$

Differentiating (4) and (5) with respect to σ and making use of (7) yields the thermal wind equations,

$$\frac{\partial}{\partial t} \left(\frac{\partial u}{\partial \sigma} \right) = - \frac{\partial}{\partial \sigma} (w \cdot \nabla u) + \frac{\partial}{\partial \sigma} (fv) - R \frac{\partial T}{\partial x} \quad (8)$$

$$\frac{\partial}{\partial t} \left(\frac{\partial v}{\partial \sigma} \right) = - \frac{\partial}{\partial \sigma} (w \cdot \nabla v) - \frac{\partial}{\partial \sigma} (fu) - R \frac{\partial T}{\partial y} \quad (9)$$

Assuming that the left-hand sides of (8) and (9) are comparatively small and may be approximated by zero provides the weak constraint for Eq. (1). Equations (2) and (3) are valid if we define

$$\frac{\partial}{\partial t} \left(\frac{\partial u}{\partial \sigma} \right) = F \quad (10)$$

$$\frac{\partial}{\partial t} \left(\frac{\partial v}{\partial \sigma} \right) = G \quad (11)$$

P. Kesel and H. Lewit (1973) and J. Lewis (1972) used the same set of equations with the exception that in the following variational formalism, Lewis substituted measured momentum advection in (8) and (9).

2.2 VARIATIONAL TECHNIQUE AND ASSOCIATED EULER EQUATIONS

The necessary and sufficient condition for minimizing the functional (2) is the vanishing of its first variation (3).

$$\delta J \equiv 0$$

Substituting (8) and (9) for F and G in (3) and assuming Dirichlet conditions at the boundaries, one obtains after some manipulation (Kesel and Lewit, 1973) the following Euler equations:

$$\tilde{\alpha}(u - \tilde{u}) + \left\{ \frac{\partial v}{\partial x} + f \right\} \left\{ - \frac{\partial^2}{\partial \sigma^2} (w \cdot \nabla v) - f \frac{\partial^2 u}{\partial \sigma^2} - R \frac{\partial}{\partial \sigma} \left(\frac{\partial T}{\partial y} \right) \right\} \quad (12)$$

$$- \left\{ \frac{\partial v}{\partial y} + u \frac{\partial}{\partial x} + v \frac{\partial}{\partial y} \right\} \left\{ - \frac{\partial^2}{\partial \sigma^2} (w \cdot \nabla u) - f \frac{\partial^2 v}{\partial \sigma^2} - R \frac{\partial}{\partial \sigma} \left(\frac{\partial T}{\partial x} \right) \right\} = 0$$

$$\tilde{\alpha}(v - \tilde{v}) + \left\{ \frac{\partial u}{\partial y} - f \right\} \left\{ - \frac{\partial^2}{\partial \sigma^2} (w \cdot \nabla u) - f \frac{\partial^2 v}{\partial \sigma^2} - R \frac{\partial}{\partial \sigma} \left(\frac{\partial T}{\partial x} \right) \right\} \quad (13)$$

$$- \left\{ \frac{\partial u}{\partial x} + u \frac{\partial}{\partial x} + v \frac{\partial}{\partial y} \right\} \left\{ - \frac{\partial^2}{\partial \sigma^2} (w \cdot \nabla v) - f \frac{\partial^2 u}{\partial \sigma^2} - R \frac{\partial}{\partial \sigma} \left(\frac{\partial T}{\partial y} \right) \right\} = 0$$

$$\begin{aligned} \tilde{\beta}(T - \tilde{T}) + R \left\{ \frac{\partial}{\partial \sigma} \left[\frac{\partial}{\partial x} (w \cdot \nabla u) + \frac{\partial}{\partial y} (w \cdot \nabla v) - \frac{\partial}{\partial x} (fv) \right. \right. \\ \left. \left. + \frac{\partial}{\partial y} (fu) \right] \right\} + R^2 \left\{ \frac{\partial^2 T}{\partial x^2} + \frac{\partial^2 T}{\partial y^2} \right\} = 0 \end{aligned} \quad (14)$$

$\tilde{\alpha}$ and $\tilde{\beta}$ are defined by,

$$\tilde{\alpha} =: \frac{\alpha}{\gamma} \quad \tilde{\beta} =: \frac{\beta}{\gamma}$$

These up to the fourth order non-linear set of partial differential equations are solved by sequential relaxation techniques.

2.3 FINITE DIFFERENCING SCHEME AND RELAXATION TECHNIQUE

The finite differencing scheme is set up for a half-mesh 29 X 29 grid over the European-Mediterranean area as shown in Figure 1. The input data is interpolated to half-mesh from the operational FNWC 12-level analysis, the wind components being the geostrophic wind components derived from the height fields at each level. Equations (12) through (14) are solved at each of the 10 interior levels utilizing the sequential relaxation technique. In the case of Eq. (14) -- Helmholtz type of equation -- an over-relaxation factor of .6 is introduced. Equations (12) and (13) lead to the following general type of equation for the (m+1)th approximation of u and v respectively.

$$f_1 \{ \phi_{ij}^m - \phi_{ij}^{m+1} \} + f_2 \{ (\phi_{ij}^m)^2 - (\phi_{ij}^{m+1})^2 \} = R_{ij}^m \quad (15)$$

This equation is linearized giving:

$$\phi_{ij}^{m+1} = \{ f_1 \phi_{ij}^m + 2f_2 (\phi_{ij}^m)^2 - R_{ij}^m \} / \{ f_1 + 2f_2 \phi_{ij}^m \} \quad (16)$$

Equations (12) through (14) are a simultaneous set of equations. To be more economical with respect to computer storage and computational time, Eqs. (12) through (14) are solved on vertical x- σ planes of the computational grid.

(1,1)

(1,29)

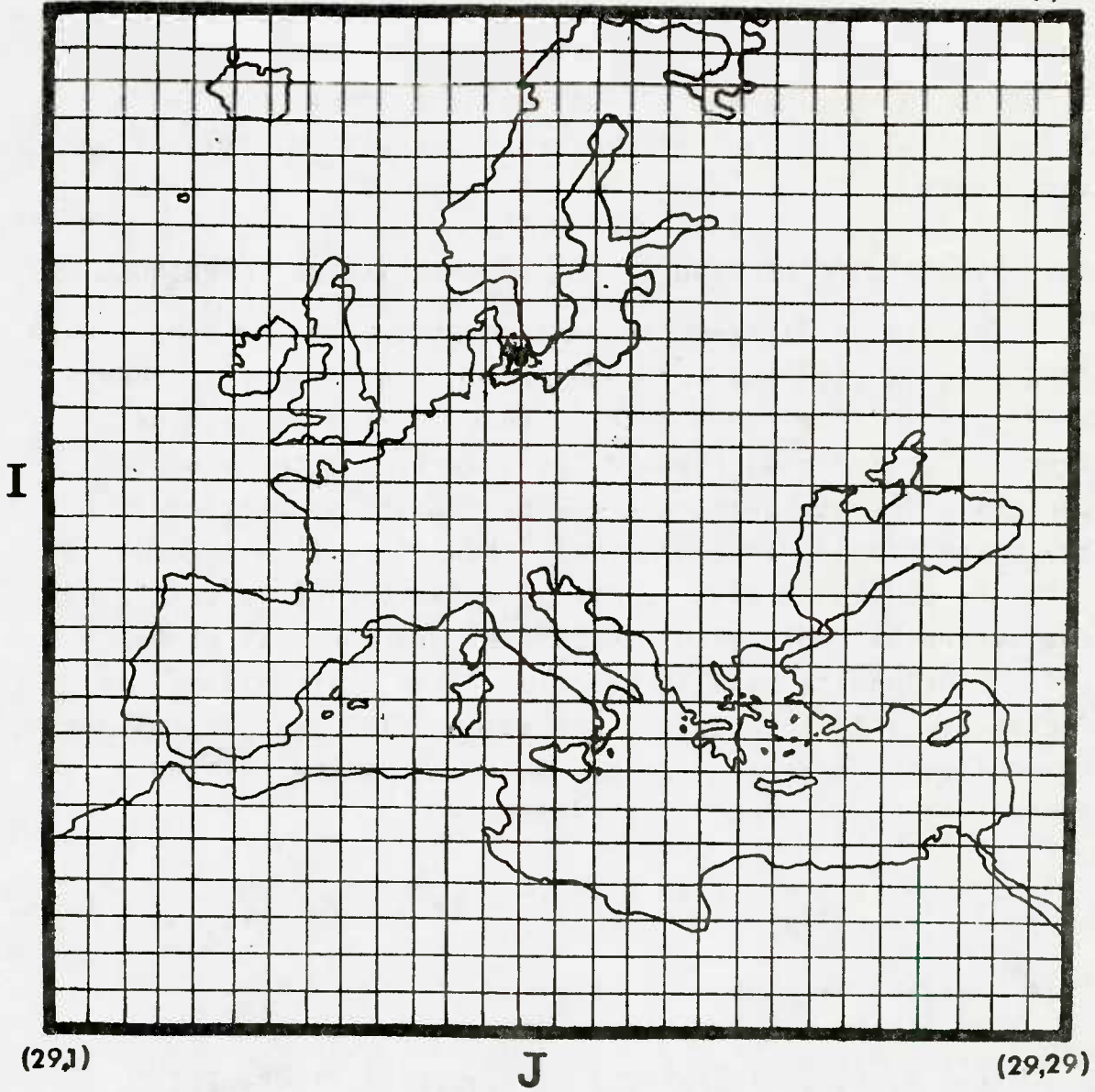


Figure 1. European-Mediterranean area (half-mesh FNWC grid)

The convergence criteria for the three equations are that in their finite difference form, the respective residuals are less than 1 at each grid point. The simultaneous set converges toward a stable solution for T, u, and v if the root mean square deviation between the solutions of the last 3 successive runs through the atmosphere is less than .005. A number of test-runs were made to assure that this condition is sufficient.

3. SOLUTIONS

To ensure that a stable solution achieved under the above mentioned conditions is physically significant, some properties of the solutions have to be discussed.

3.1 CONVERGENCE OF THE FINITE DIFFERENCE APPROXIMATION

Since Eqs. (12) through (14) are a simultaneous set of non-linear partial differential equations, no general convergence criteria could be found. However, a stable solution was achieved with the finite difference approximation described in Section 2.3. All the following tests have been made taking the FNWC routine analysis for March 16, 1972, 0000Z, as the initial guess at all grid points interpolated to half-mesh grid distance. In order to check convergence and the rate of convergence, the standard deviations σ_T , σ_W for temperature and wind velocity respectively were calculated over the whole domain after each iteration cycle.

$$\sigma_T = \left[\frac{1}{N} \left\{ \sum_{i,j,k} (\tilde{T}_{i,j,k} - T_{i,j,k})^2 \right\} \right]^{\frac{1}{2}}, \quad (17)$$

$$\sigma_W = \left[\frac{1}{N} \left\{ \sum_{i,j,k} (|\tilde{W}|_{i,j,k} - |W|_{i,j,k})^2 \right\} \right]^{\frac{1}{2}}. \quad (18)$$

$N = 25 \times 25 \times 10$, i and j range from 1 to 25, and k ranges from 1 to 10. Figures 2 and 3 and Table 1 show the results for a number of differently chosen weights α and β . Although the convergence behavior is basically similar to that which Sasaki (1970b) found investigating shallow water waves, it has not been necessary to introduce auxiliary damping factors into the system in order to prevent the iterating process from diverging. Figures 2 and 3 show that σ_T and σ_W converge

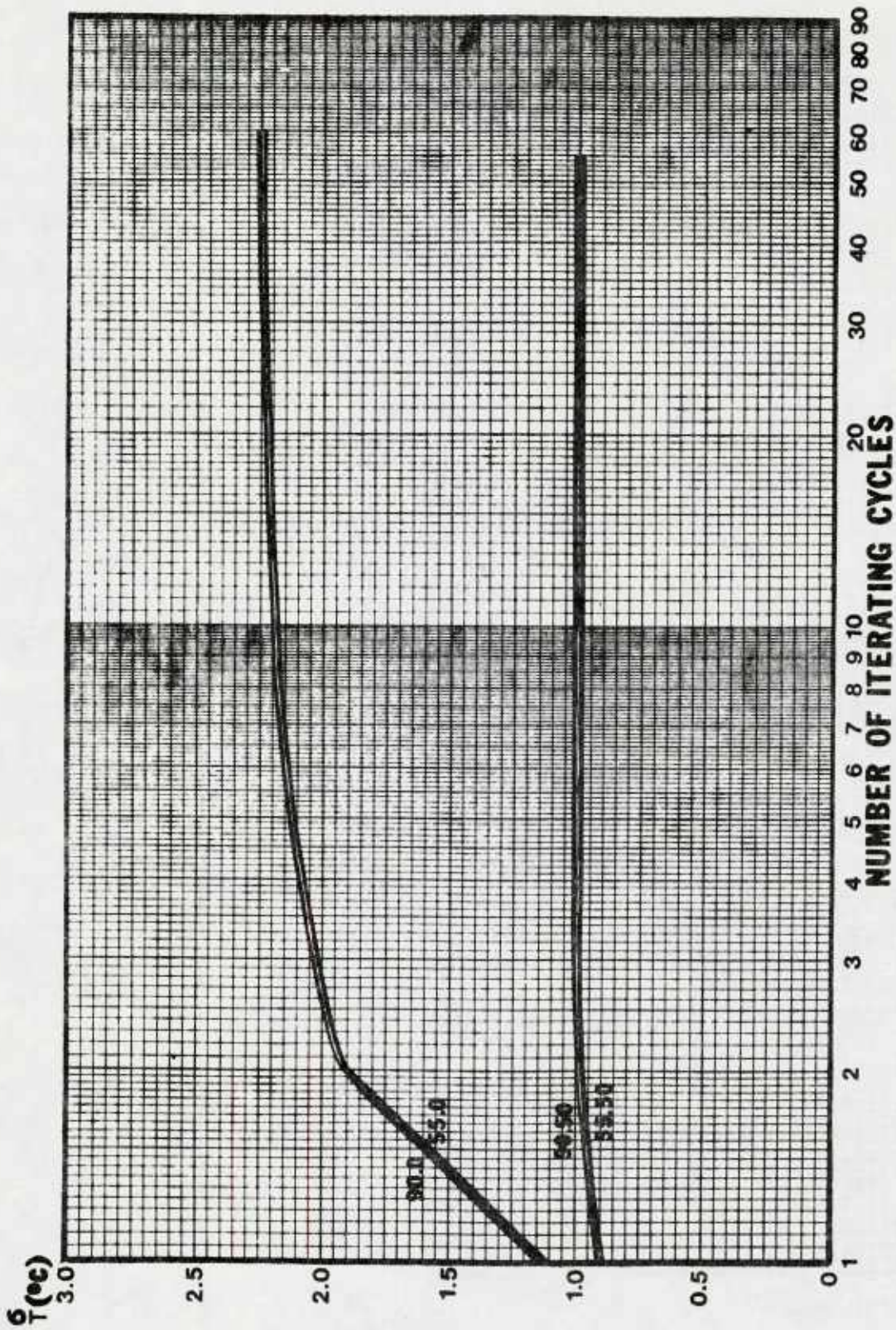


Figure 2. σ_T RMS deviation between initial guess and NVA temperature field weights α , β .

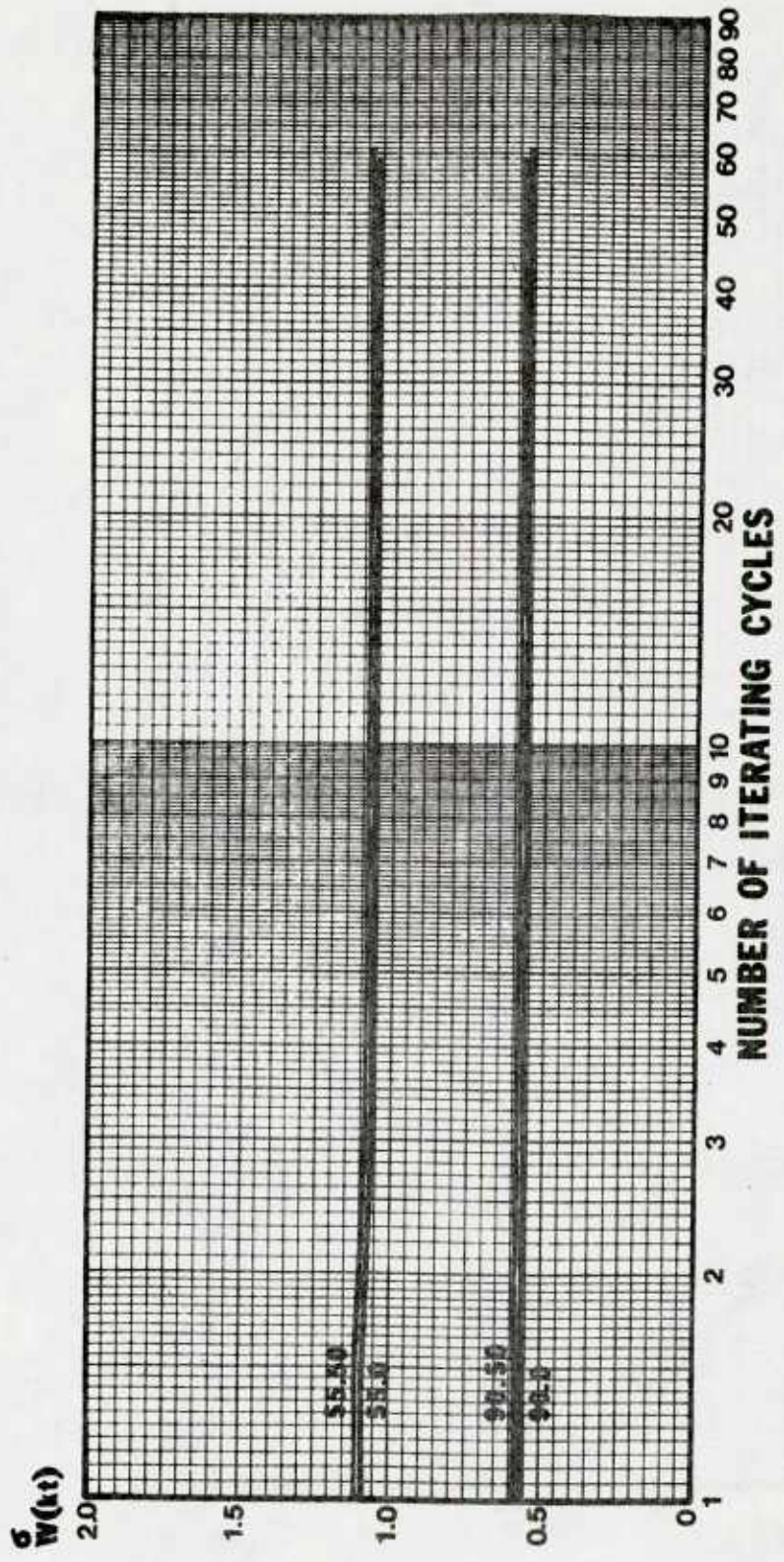


Figure 3. σ_W RMS deviation between initial guess and NVA wind field weights $\tilde{\alpha}$, $\tilde{\beta}$

Table 1. RMSD between initial guess and NVA temperature and wind fields.

WEIGHTS α β	55,0		90,0		90,50		55,50	
	σ_T	σ_W	σ_T	σ_W	σ_T	σ_W	σ_T	σ_W
Cycles								
1	1.25	1.19	1.26	.68	.80	.70	.79	1.21
2	1.82	1.14	1.83	.65	.98	.67	.97	1.18
3	2.05	1.12	2.07	.64	1.00	.67	.99	1.17
4	2.17	1.12	2.18	.63	1.01	.67	1.00	1.17
5	2.23	↓	2.24	.63	1.01	↓	1.00	1.17
6	2.27		2.28	↓	↓		1.17	
7	2.30		2.31					
8	2.32		2.33					
9	2.34		2.35					
10	2.35		2.37					
11	2.36		2.38					
12	2.38		2.39					
13	2.39		2.40					
14	2.39		2.41					
15	2.40		2.41					
16	2.41		2.42					
17	2.41		2.43					
18	2.42		2.43					
19	2.42							
20	2.42							
·								
·								
30	2.46		2.47					
·								
·								
40	2.46	2.48						
·								
·								
60	2.47	1.12	2.48	.63	1.01	.67	1.00	1.17

rapidly and steadily toward a number that obviously depends solely on the weights ($\tilde{\alpha}$, $\tilde{\beta}$) placed on the initial data. In most cases changes in σ_T and σ_W are on the order of 10^{-3} after the fifth cycle, except those cases where either the weight $\tilde{\beta}$ on the initial temperature data approaches zero or the weight $\tilde{\alpha}$ on the initial wind field data approximates a value beyond which convergence can no longer be achieved. Another interesting feature of this scheme is that the required number of iterations increases for values of $\tilde{\beta}$ approaching 0 or values of $\tilde{\alpha}$ approaching the above mentioned critical value. In addition to the above, convergence rates are faster in regions where the smallest differences occur between the initial data and the final solution.

3.2 CONVERGENCE TOWARD STABLE SOLUTIONS WITH RESPECT TO ARBITRARILY CHOSEN WEIGHTS

Sasaki (1970c) found that, in using the linear advection equation as weak constraint in the NVA, convergence of the solution depends on the ratio between the weight on the input data and the weight on the dynamical constraint. The same behavior could be anticipated in this case, so several runs have been carried out with arbitrarily chosen weights $\tilde{\alpha}$ and $\tilde{\beta}$. Figure 4 shows the domain in an $\tilde{\alpha}$ - $\tilde{\beta}$ -plane where a converging solution could be obtained; an "x" marks the spot where successful convergence has been achieved and no stable solution could be found with weight combinations marked with 0. It is interesting to see that the value of $\tilde{\beta}$ seems to have no influence on convergence, whereas $\tilde{\alpha}$ has to be chosen larger than a critical value to obtain converging solutions. This is valid in the domain shown in Figure 4, but runs have been made with considerably higher values of $\tilde{\beta}$ still resulting in convergent solutions with slightly lower values of $\tilde{\alpha}$ than

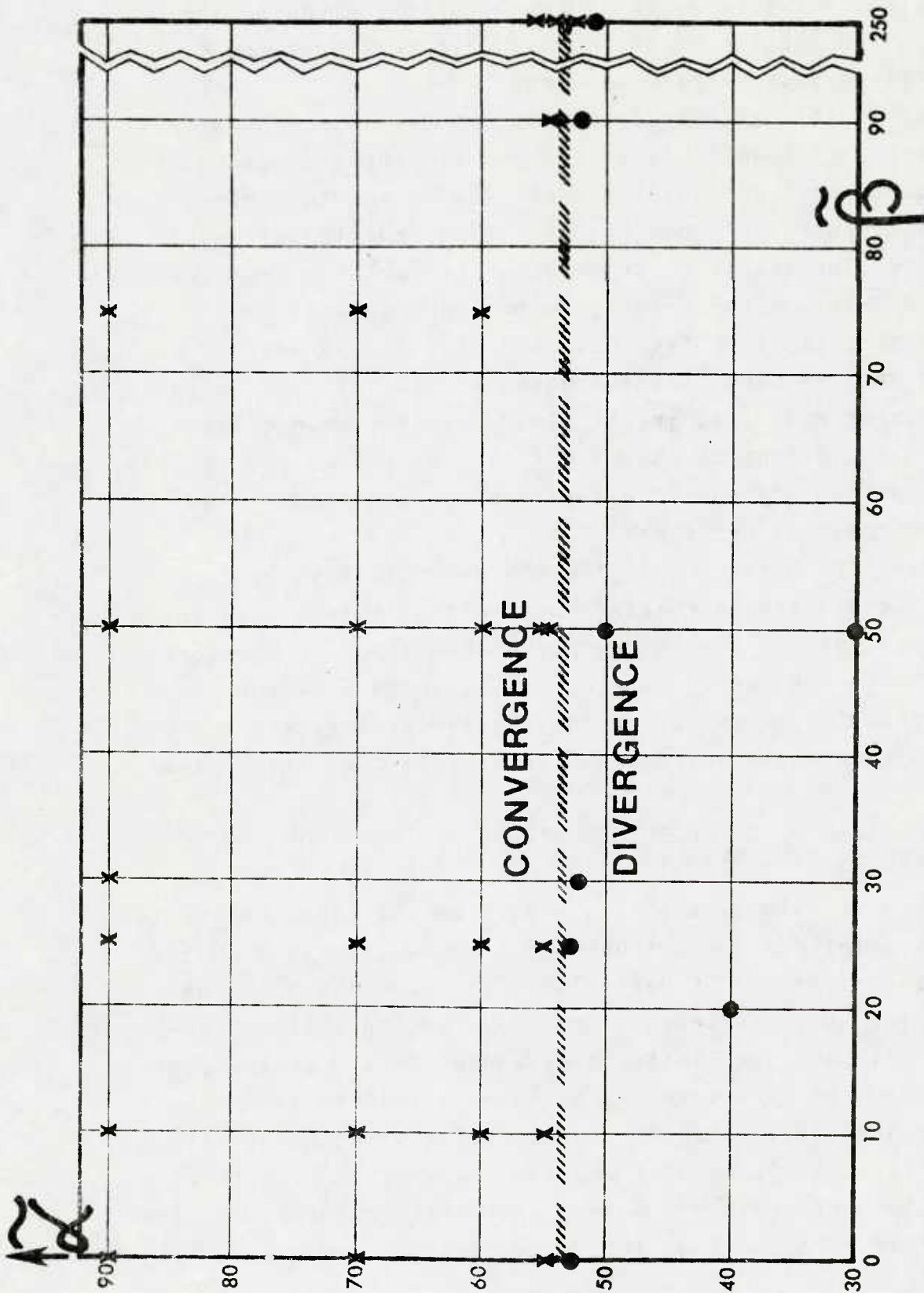


Figure 4. Domain of convergence and divergence

the critical value shown in Figure 5. The choices of the weights $\tilde{\alpha}$ and $\tilde{\beta}$ beyond that shown in Figure 4 left the initial fields essentially unchanged.

Some additional characteristics of the solutions within the domain are shown in Figures 5 and 6. The standard deviation between the initial guess fields and the output NVA has been computed according to Eqs. (17) and (18) with $j=3$ and $N=250$. The isopleths shown were interpolated from the data calculated at the points x shown in Figure 4.

It is easily seen from Figure 4 that as the weights on the observational analysis increase, the variation from this field becomes much less in the final solution, e.g., large values of the weight on the wind field ($\tilde{\alpha}$) allows the temperature fields to vary considerably, whereas the wind fields remain essentially unchanged.

It should be noted that the RMS deviations shown in Figures 5 and 6 are calculated on a vertical plane next to the boundary of the domain, but have been found to be representative for the entire domain. In order to show some of the characteristics in more detail, observational analyses and solutions are presented and discussed in the next section.

3.3 DISCUSSION OF DIFFERENT SOLUTIONS DERIVED FROM DIFFERENT SETS OF WEIGHTS

The observational analysis should be described before the different solutions are discussed. The analysis is from the 0000Z observations of 16 March 1972, as represented by the FNWC routine analysis schemes and shown in Figure 7. Figures 8 through 11 show the limited area and upper air analysis (for location of the systems refer to Figure 1). From the analysis it can be seen that a European anticyclone stretches to the highest tropospheric levels; upper-air low-pressure systems are located over southwest Europe and northern Egypt; and the southeastern portion of an intensive (945 mb) low pressure

vortex is present over the North Atlantic. The corresponding 925-, 700-, and 400-mb temperature and isotach charts are labeled "initial guess" in the sets of figures shown as Figures 12 through 29. These figures also show the NV analysis for two different sets of weights. Without going into details, the following can be said:

The technique seems to straighten out many of the detailed features the initial guess temperature fields provide, an absolutely desirable effect if raw data assembled to grid points is used. On the other hand, there is considerable shortwave noise introduced into the temperature analysis if the weights are changed more and more in favor of the dynamical constraint until a critical value is reached and the system becomes computationally unstable.

When experimenting with raw data, it may turn out that a heavy weight on the dynamical constraint is more advantageous in data-sparse areas, in which case a smoothing operator could possibly be added to Eq. (2) or run over the final solution.

The isotach charts do not show any significant differences compared to the initial guess except at 925 mb where the velocity gradient belonging to the North Atlantic low-pressure system gets unreasonably steep in the NV analysis when the weight on the initial data is decreased.

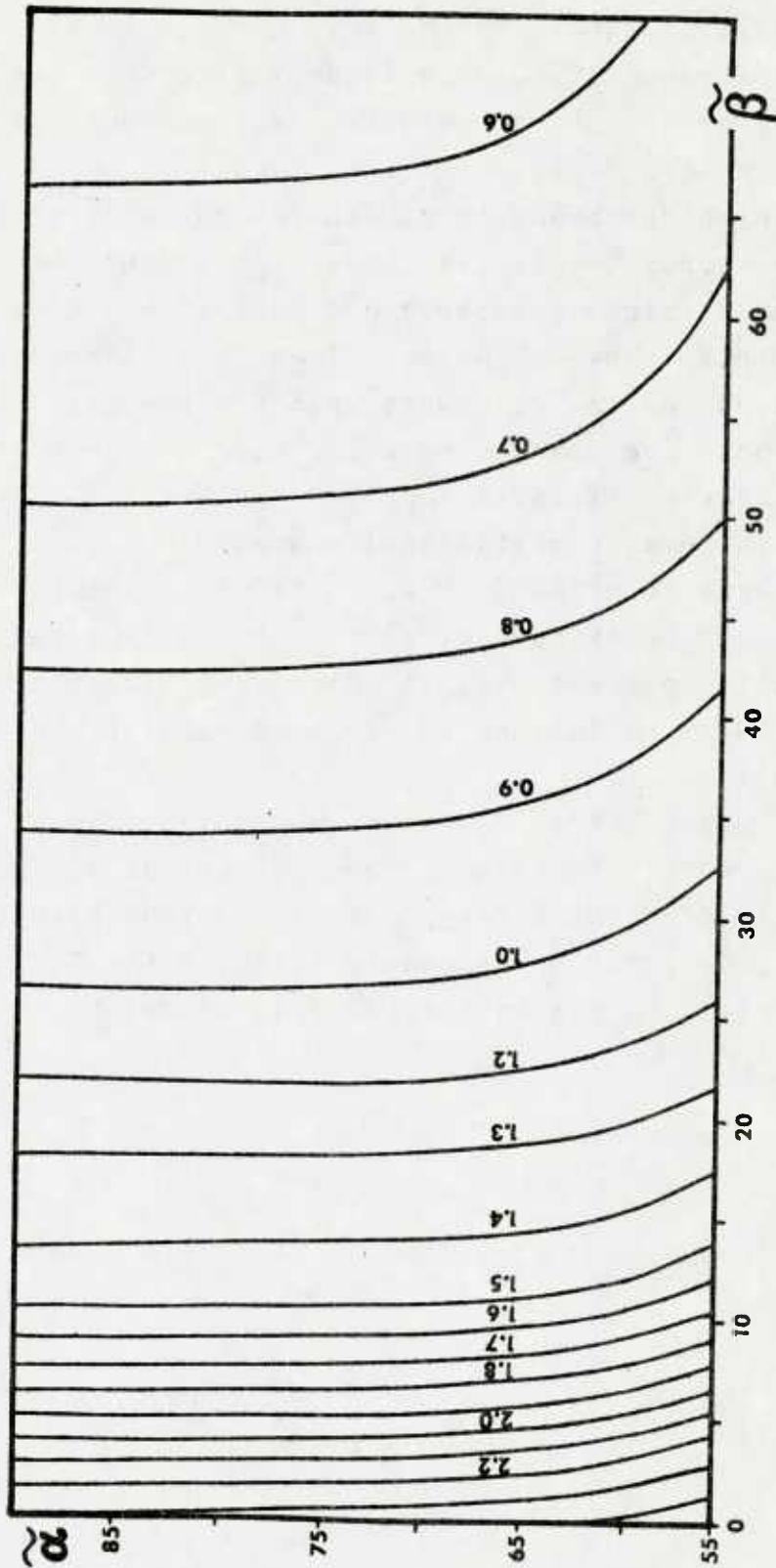


Figure 5. Isopleths of RMSD ($^{\circ}\text{C}$) between initial guess and NVA temperature field

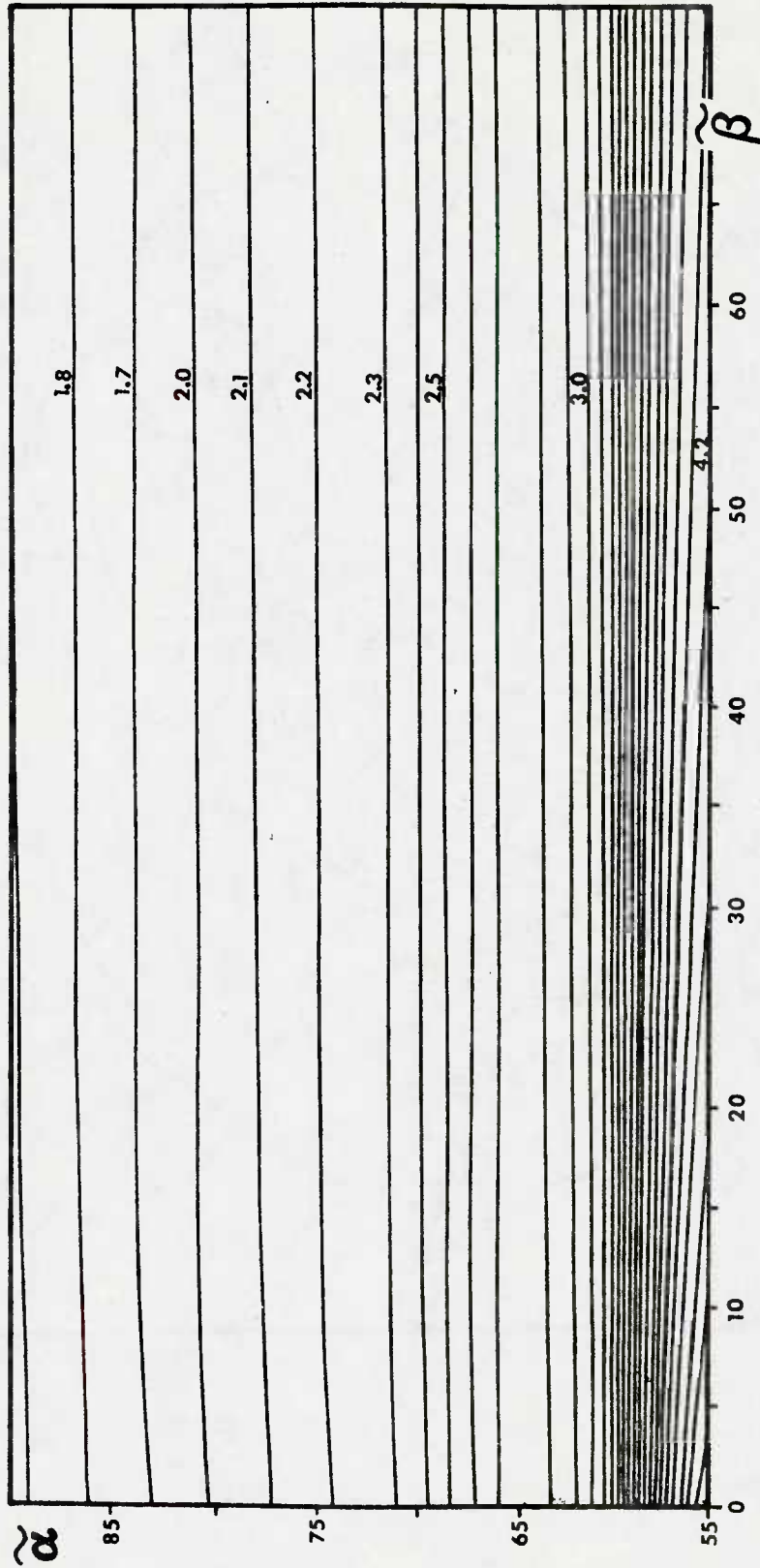


Figure 6. Isopleths of RSMD (kt) between initial guess and NVA wind field

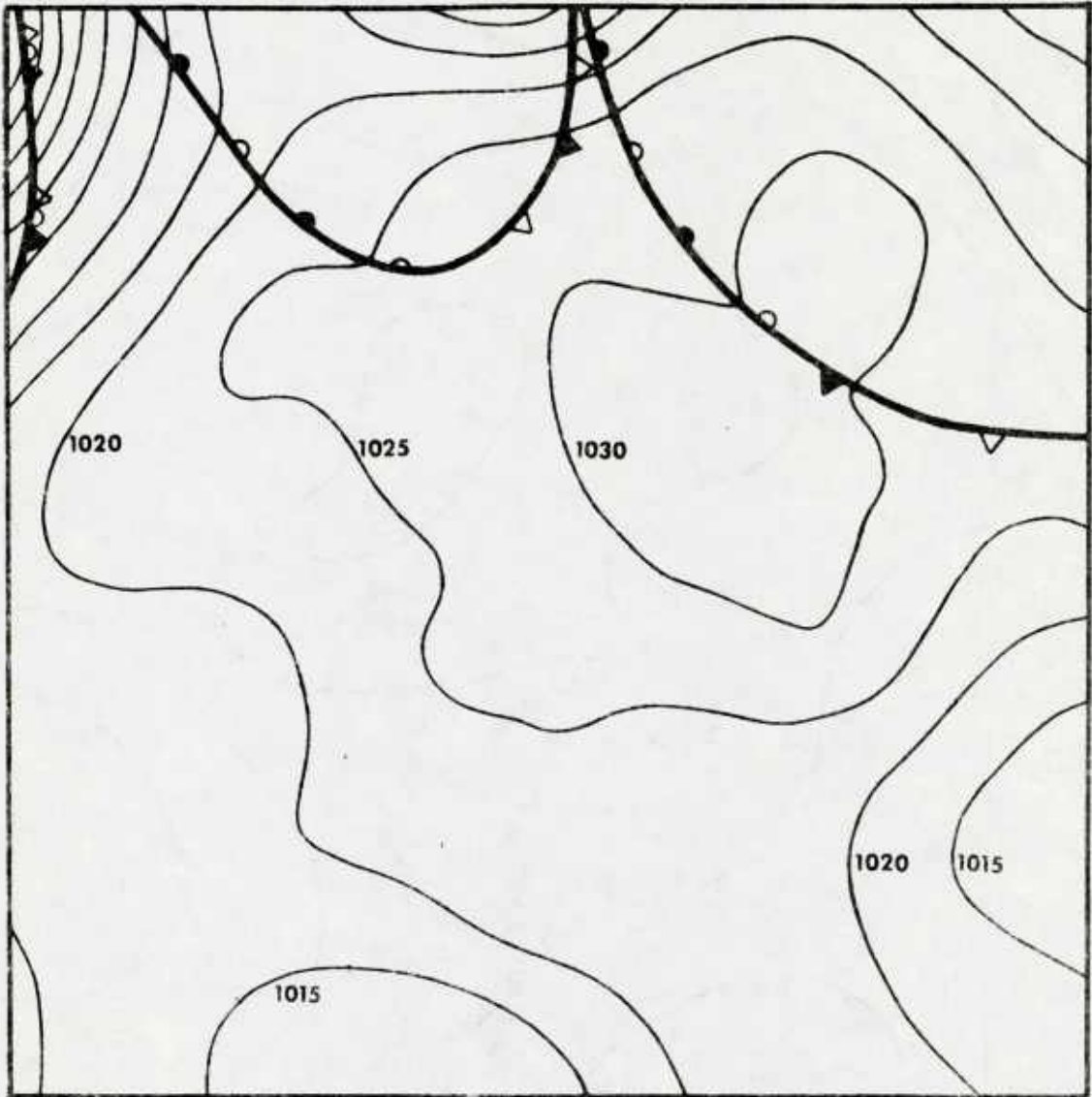


Figure 8. Surface pressure, 16 March 1972, 0000Z

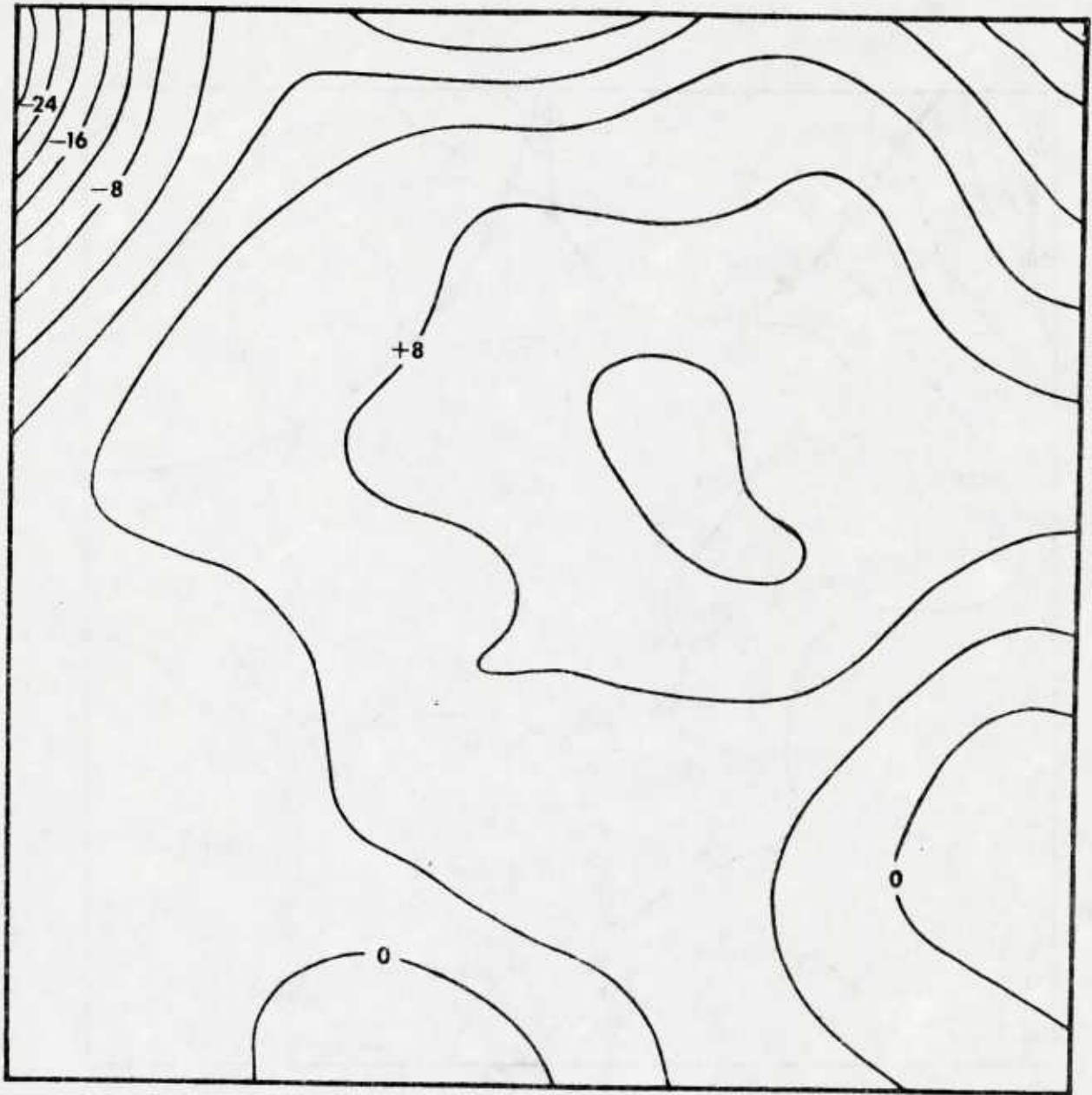


Figure 9. D values at 925 mb (in geopotential decameters)

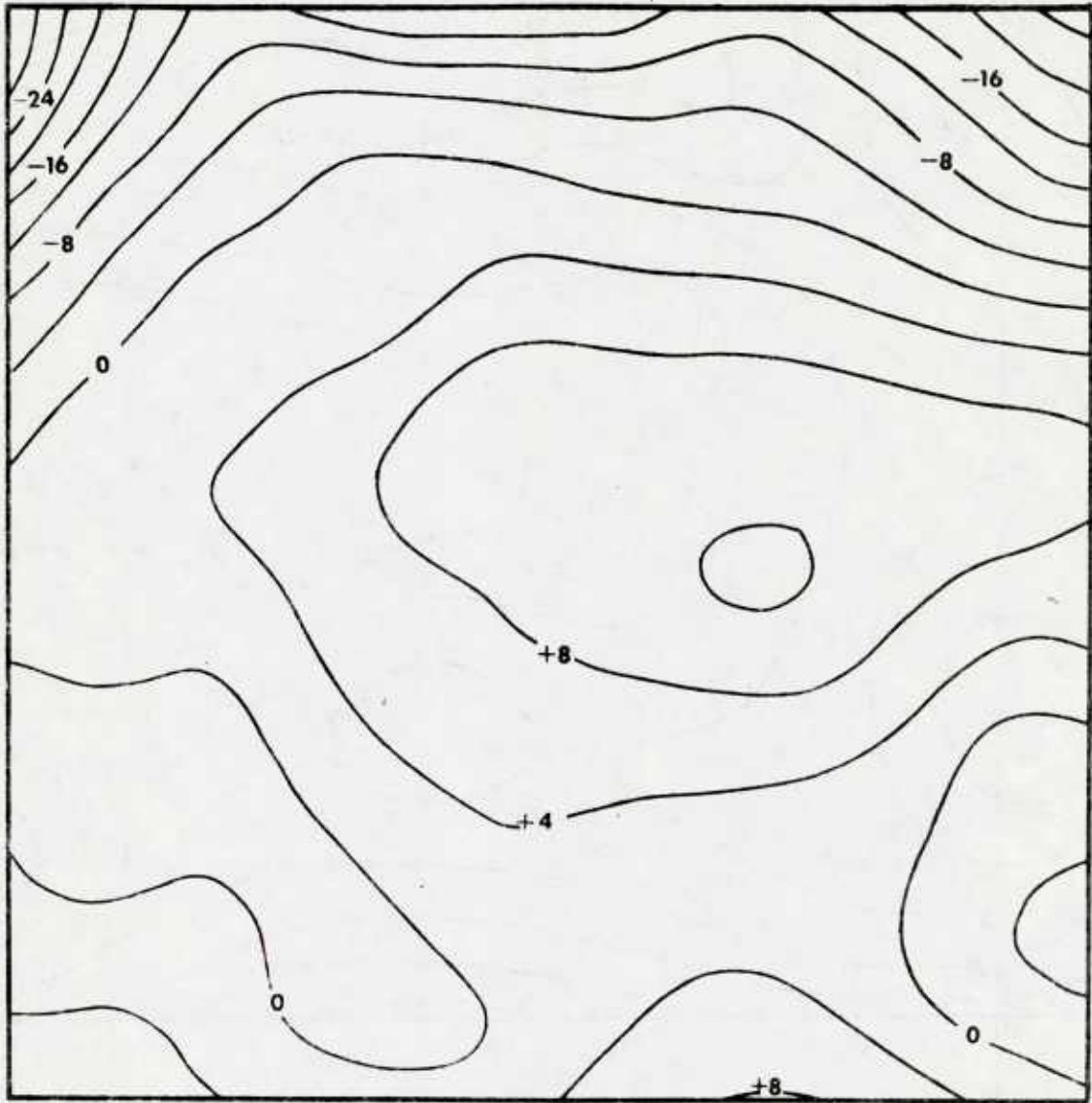


Figure 10. D values at 700 mb (in geopotential decameters)

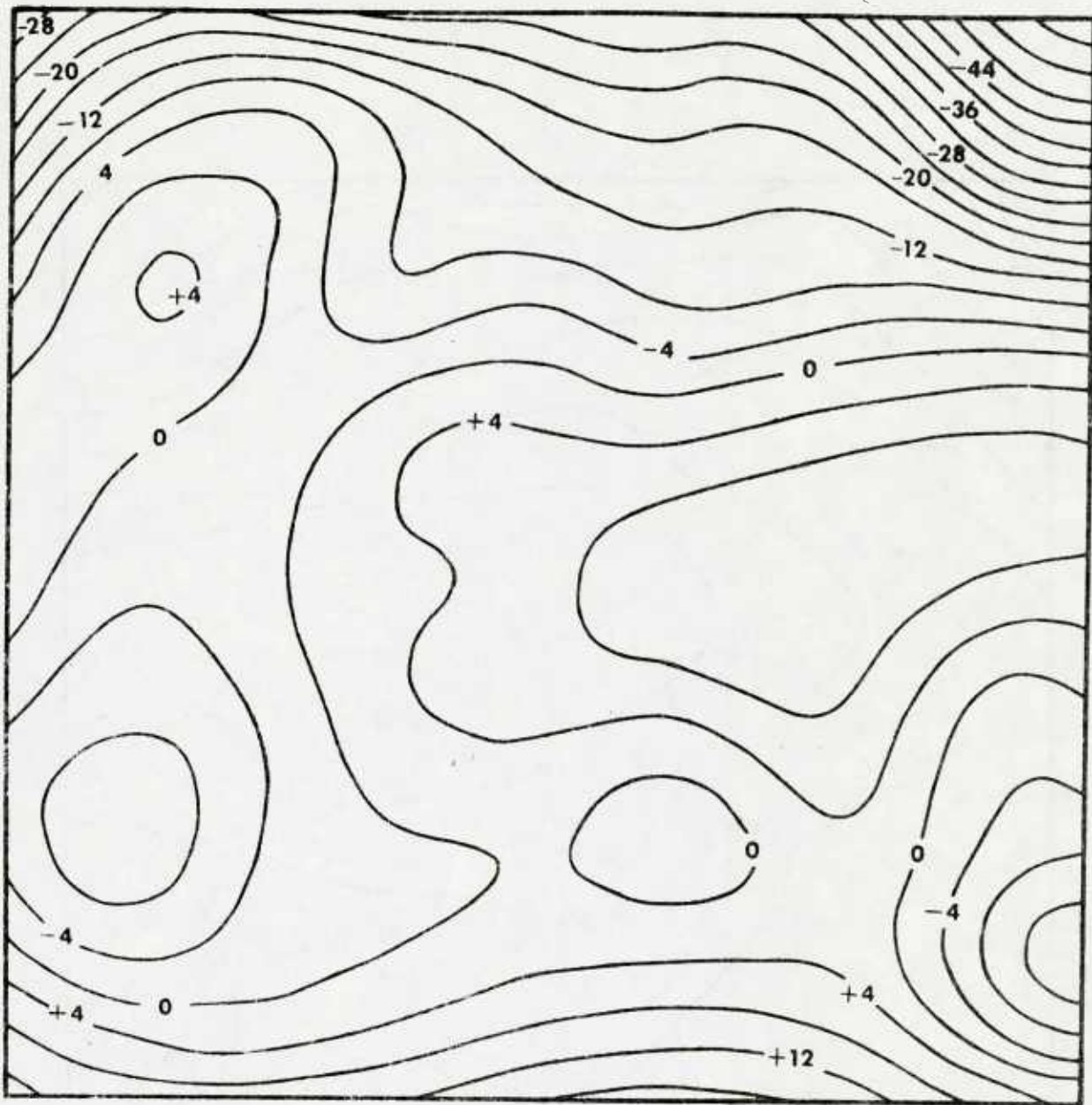


Figure 11. D values at 400 mb (in geopotential decameters)

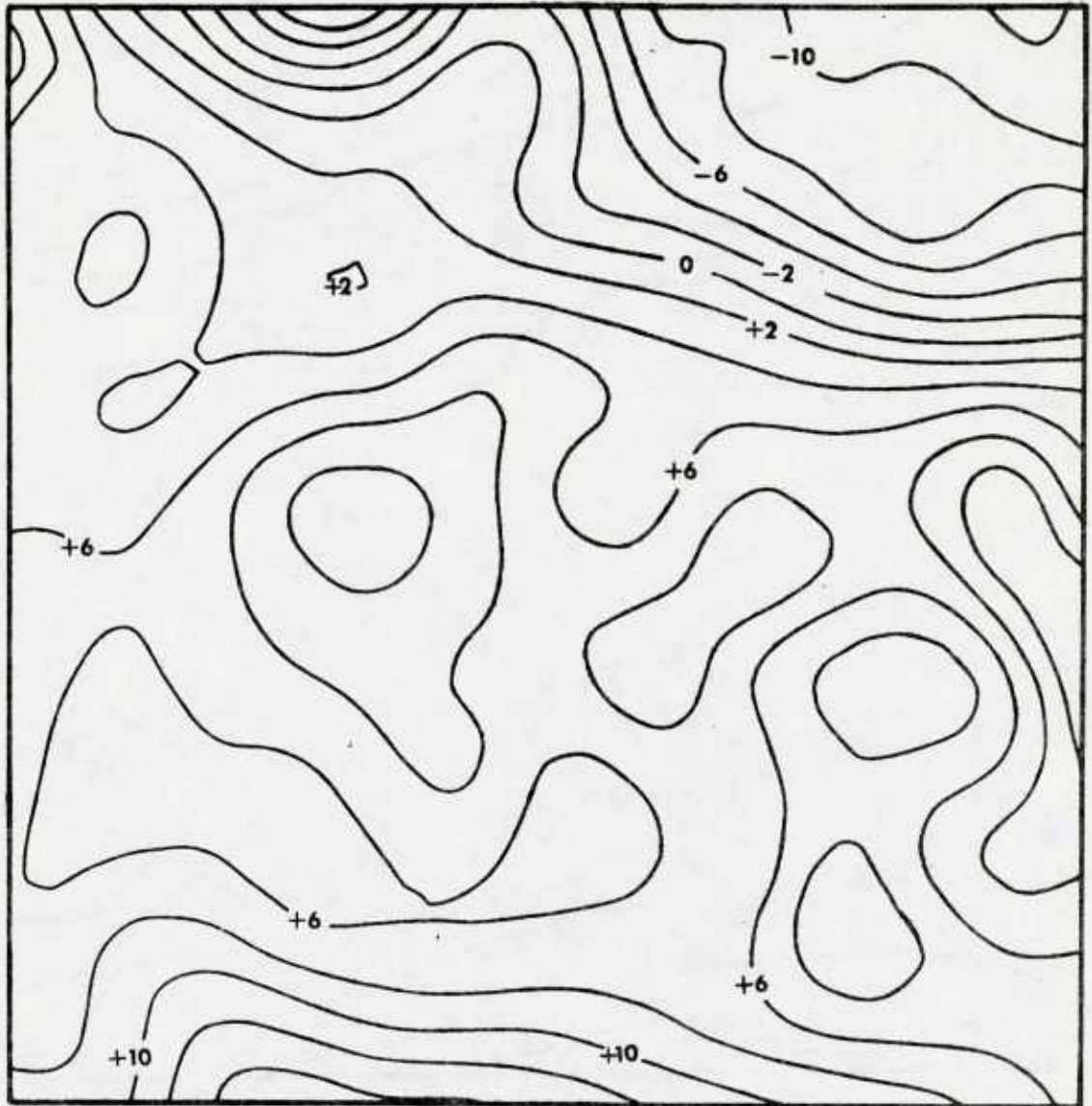


Figure 12. Initial guess temperature fields ($^{\circ}\text{C}$) at 925 mb

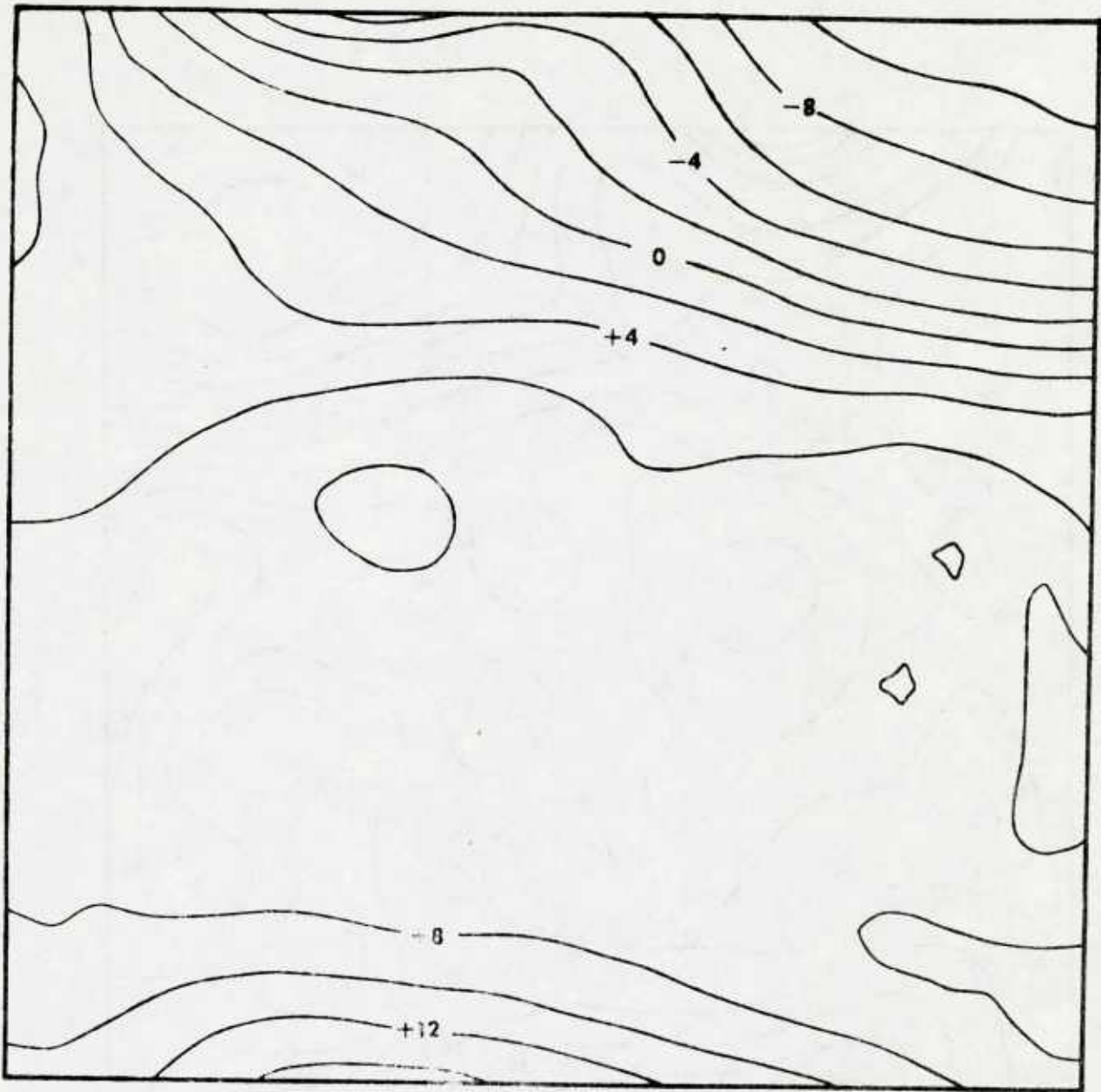


Figure 13. NVA temperature fields ($^{\circ}\text{C}$) at 925 mb, weights
 $(\alpha, \beta) = (60, 25)$

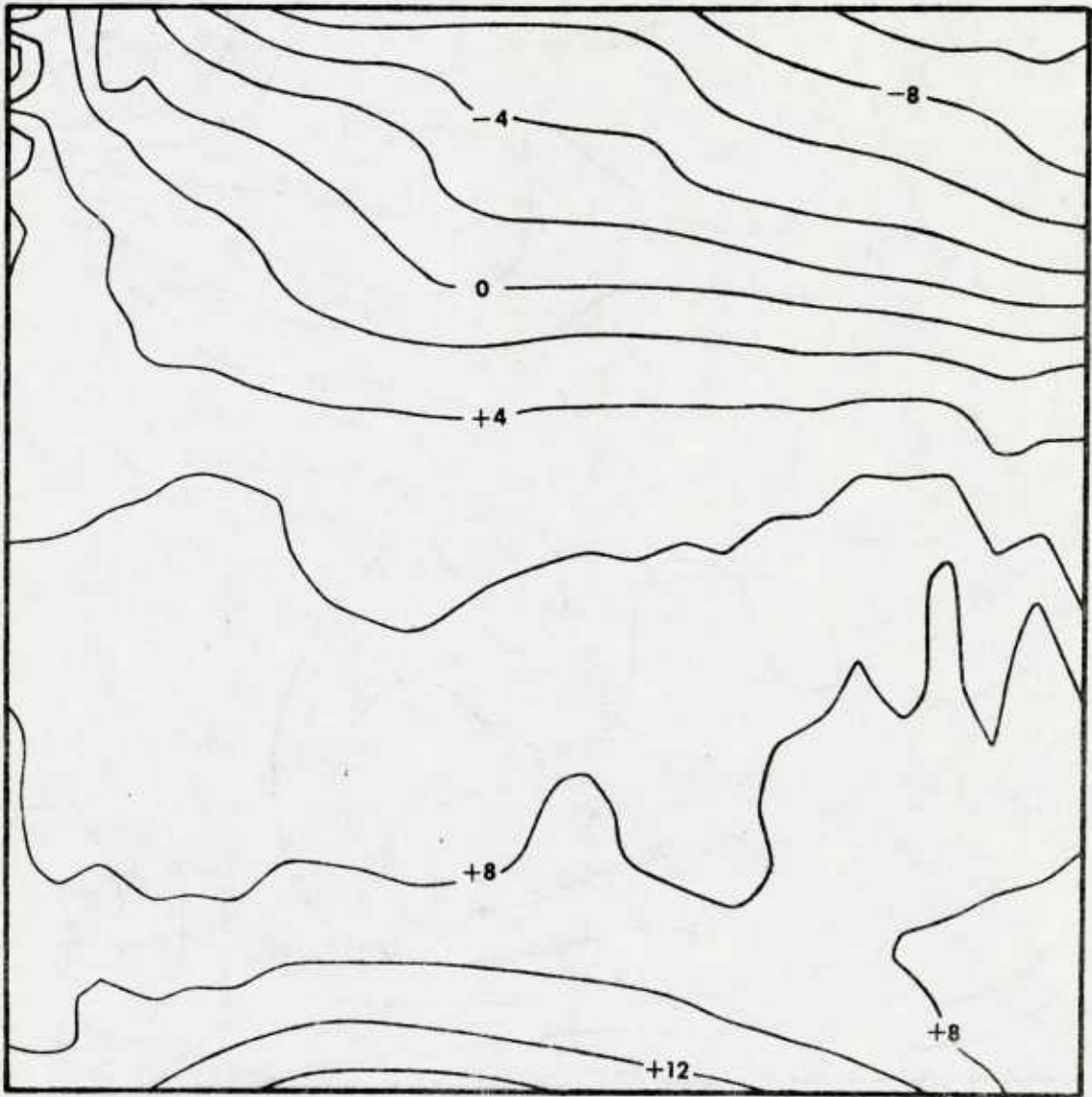


Figure 14. NVA temperature fields ($^{\circ}\text{C}$) at 925 mb, weights $(\tilde{\alpha}, \tilde{\beta}) = (55, 0)$

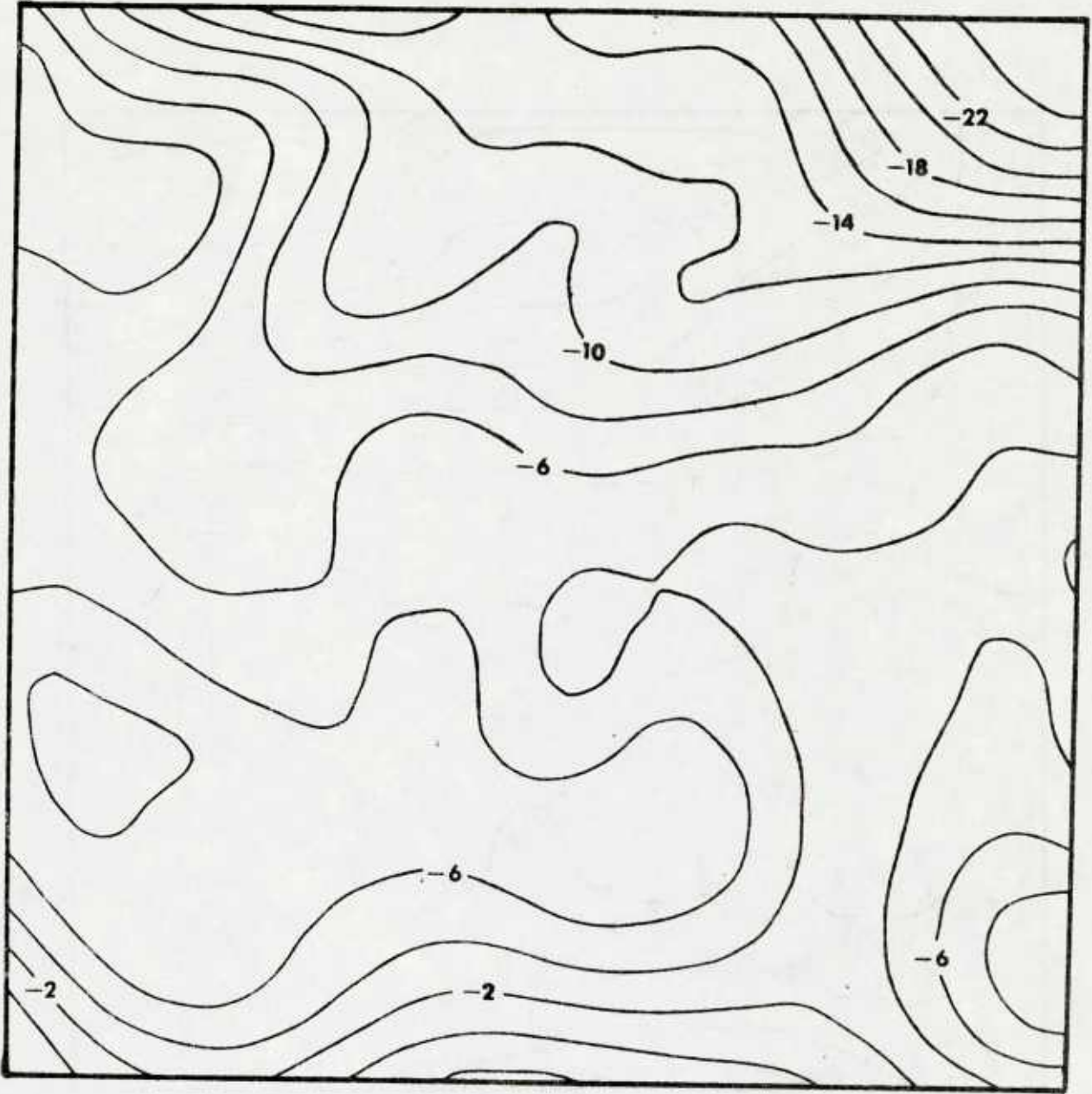


Figure 15. Initial guess temperature fields ($^{\circ}\text{C}$) at 700 mb

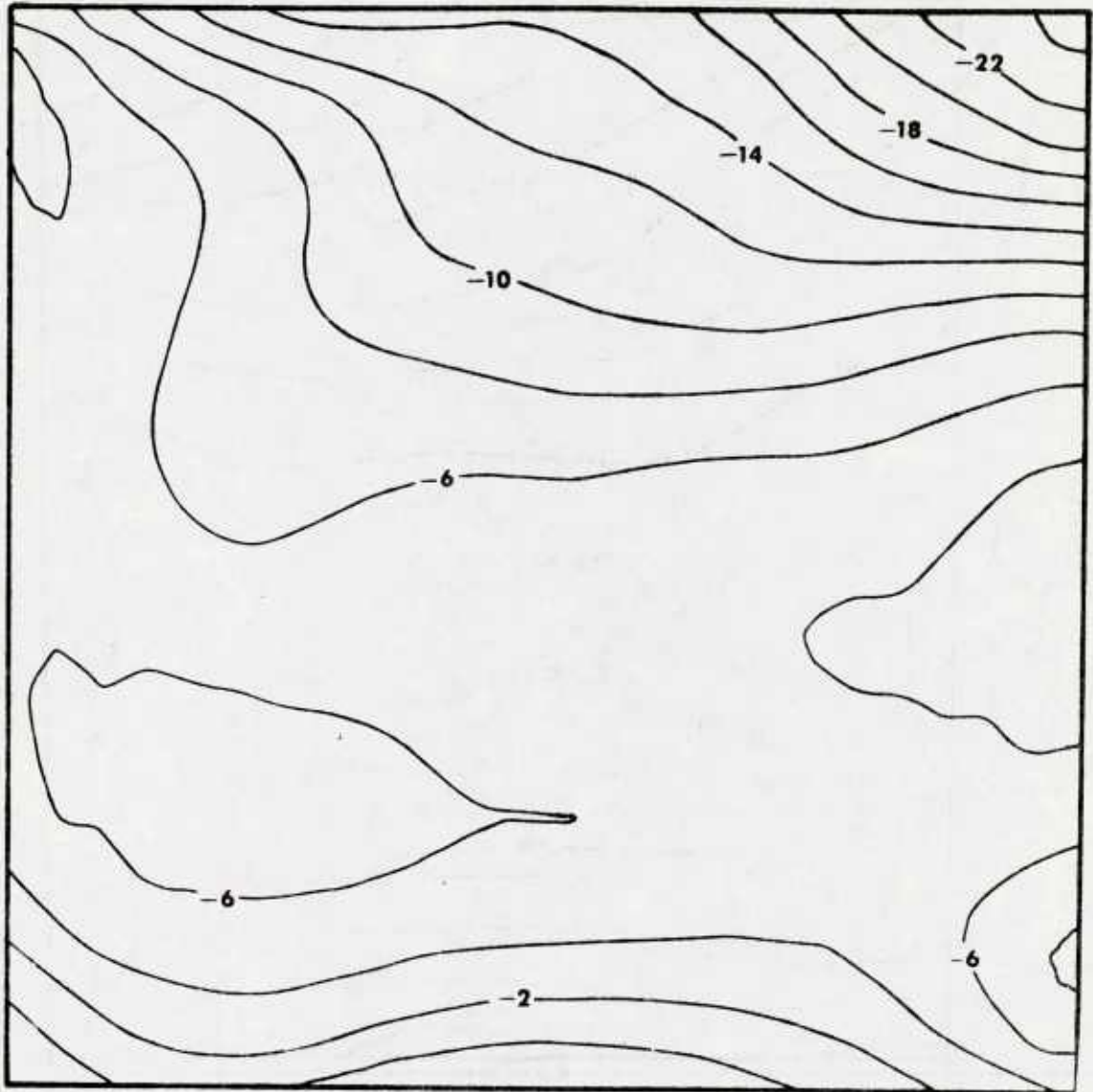


Figure 16. NVA temperature fields ($^{\circ}\text{C}$) at 700mb, weights
 $(\alpha, \beta) = (60, 25)$

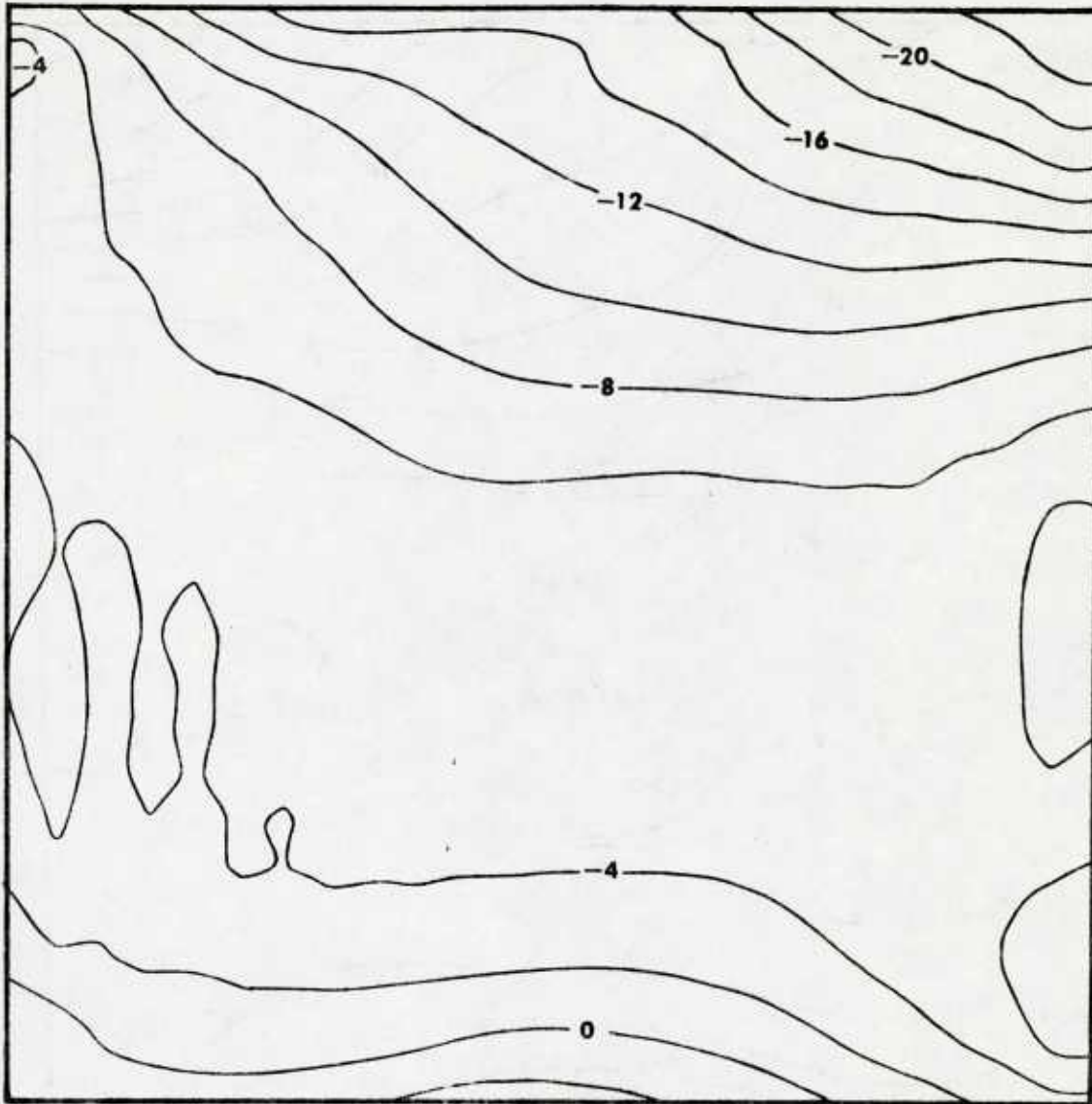


Figure 17. NVA temperature fields ($^{\circ}\text{C}$) at 700 mb, weights
 $(\tilde{\alpha}, \tilde{\beta}) = (55, 0)$

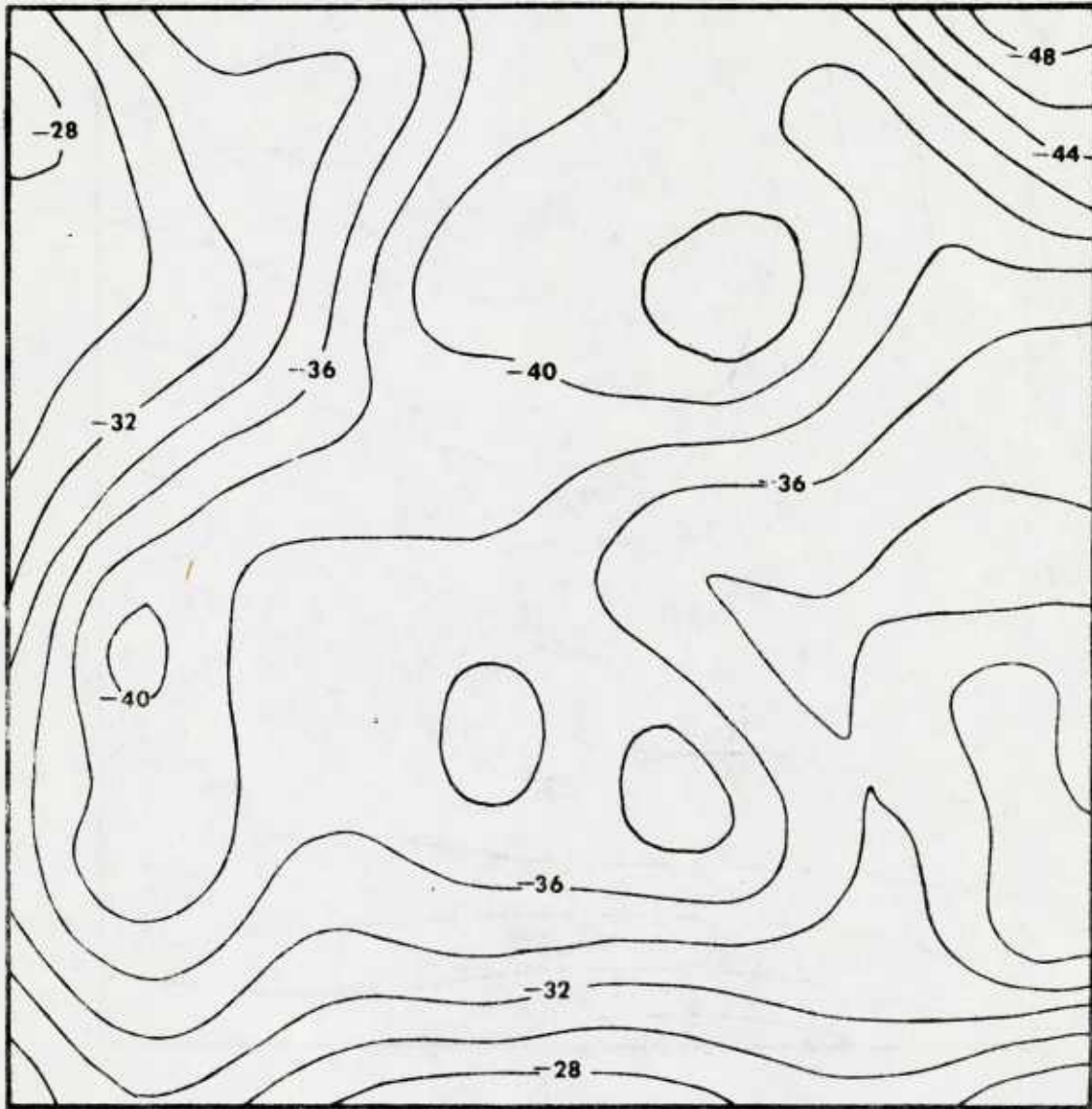


Figure 18. Initial guess temperature fields ($^{\circ}\text{C}$) at 400 mb

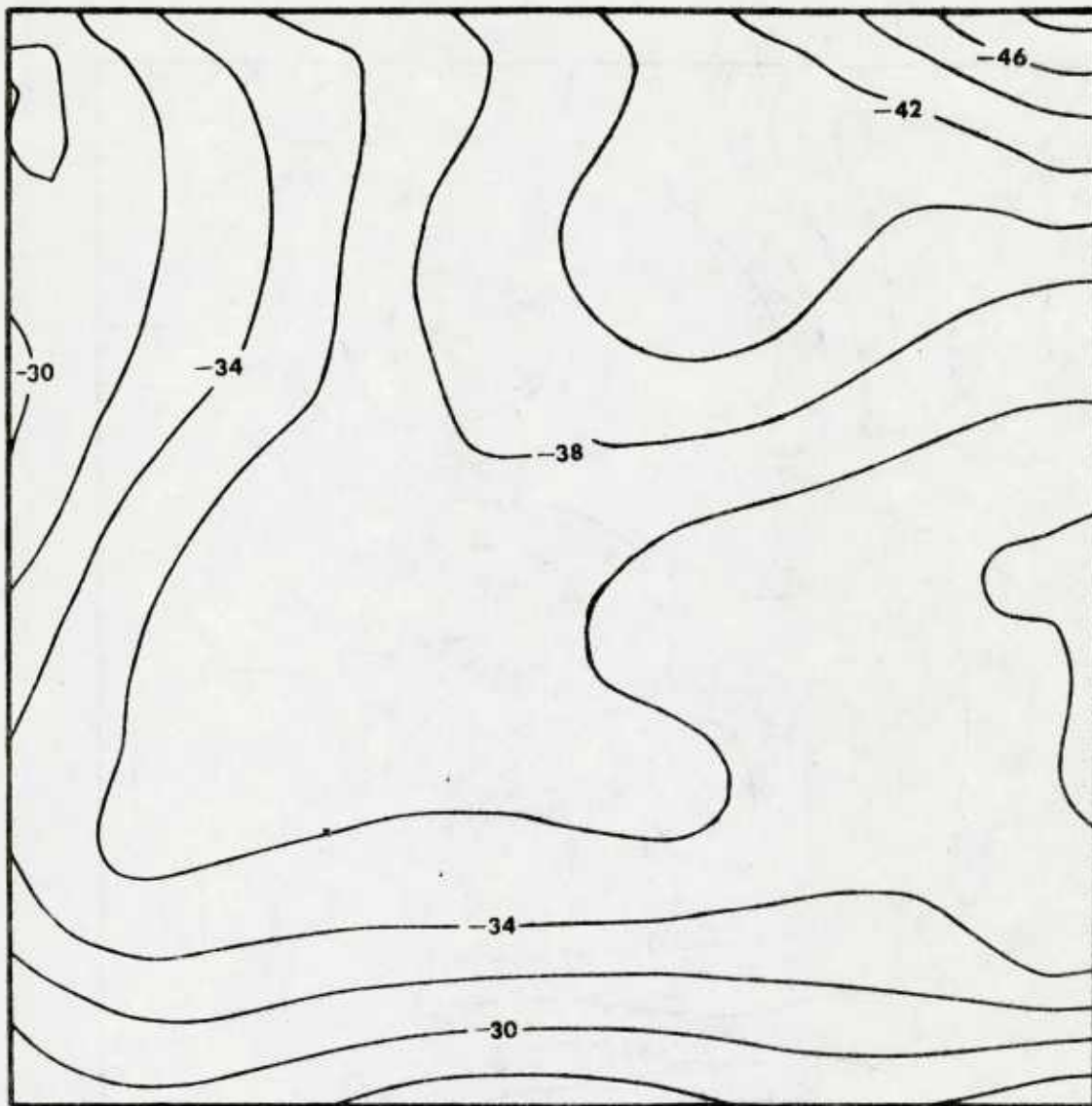


Figure 19. NVA temperature fields ($^{\circ}\text{C}$) at 400 mb, weights,
 $(\alpha, \beta) = (60, 25)$

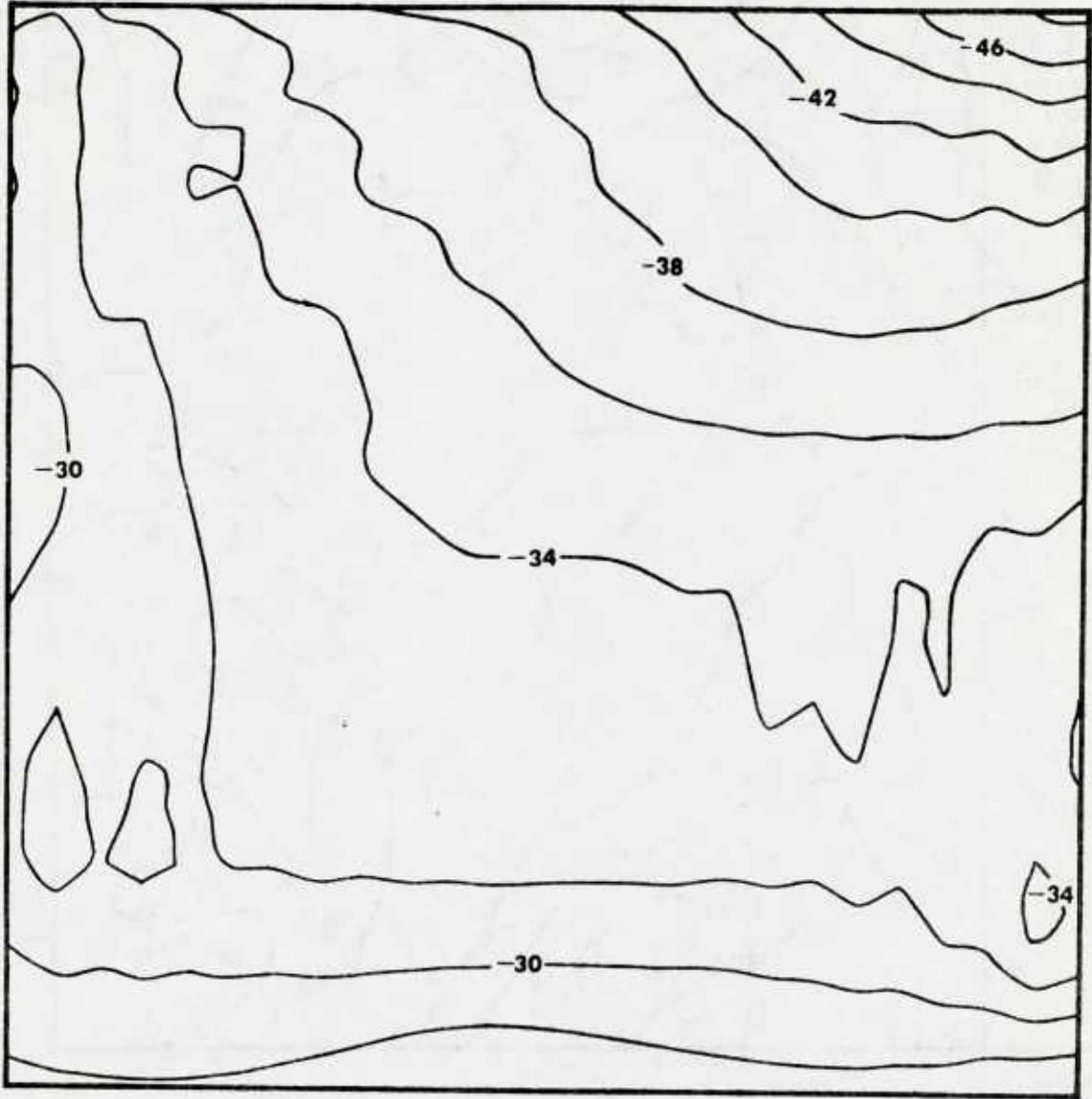


Figure 20. NVA temperature fields ($^{\circ}\text{C}$) at 400 mb, weights $(\alpha, \beta) = (55, 0)$

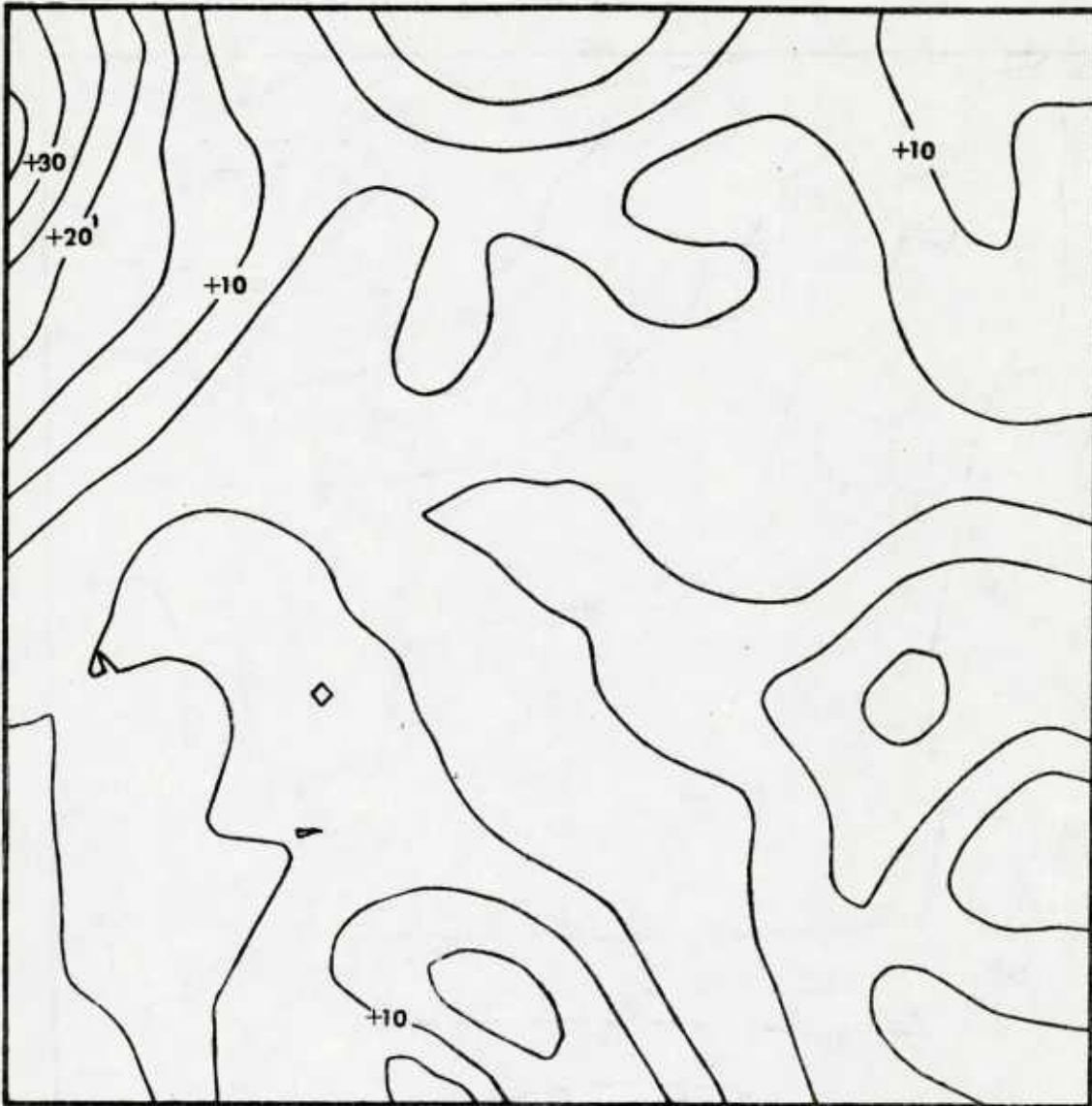


Figure 21. Initial guess isotachs (kt) at 925 mb

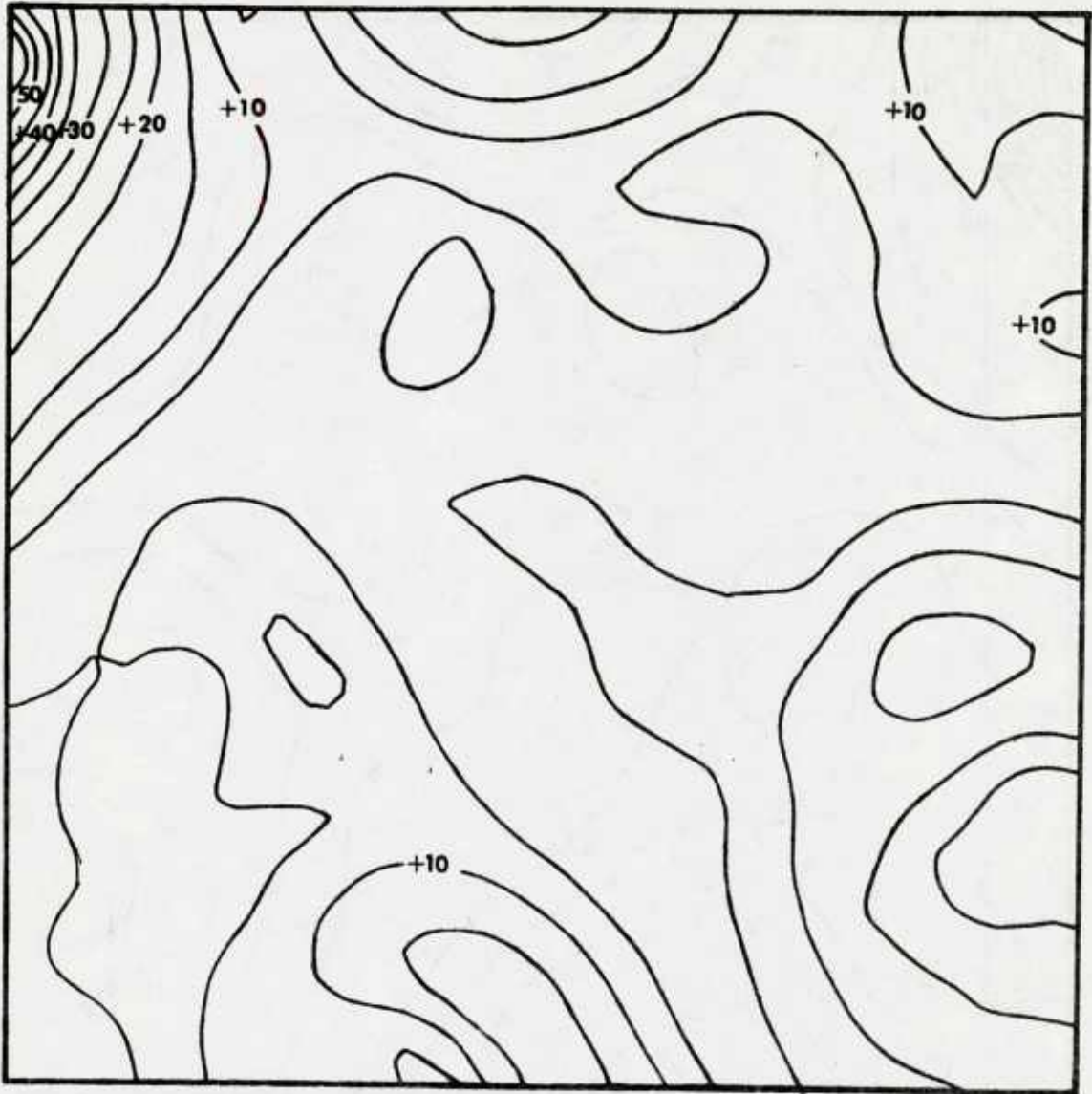


Figure 22. NVA isotachs (kt) at 925 mb, weights $(\tilde{\alpha}, \tilde{\beta}) = (60, 25)$

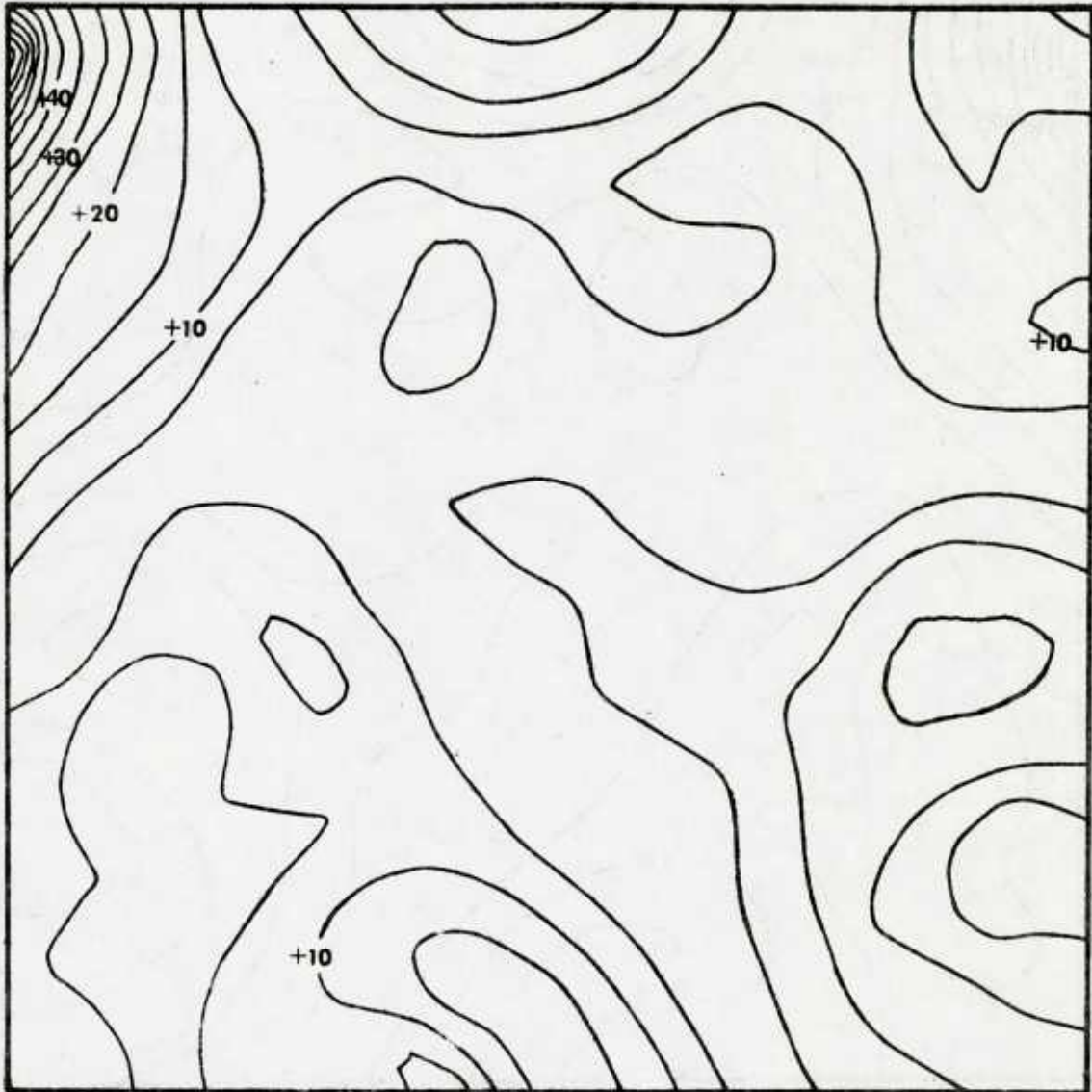


Figure 23. NVA isotachs (kt) at 925 mb, weights $(\tilde{\alpha}, \tilde{\beta}) = (55, 0)$

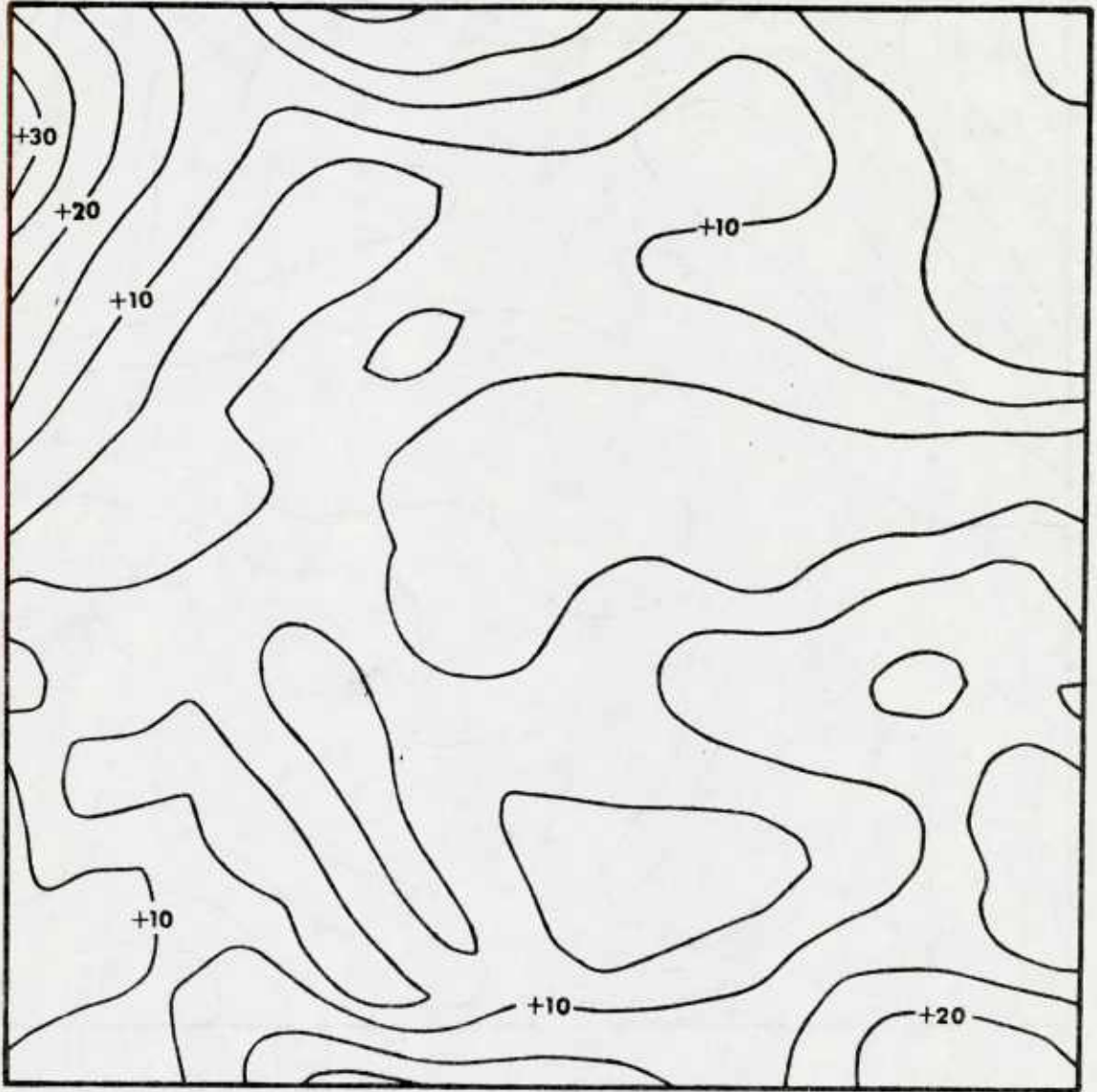


Figure 24. Initial guess isotachs (kt) at 700 mb

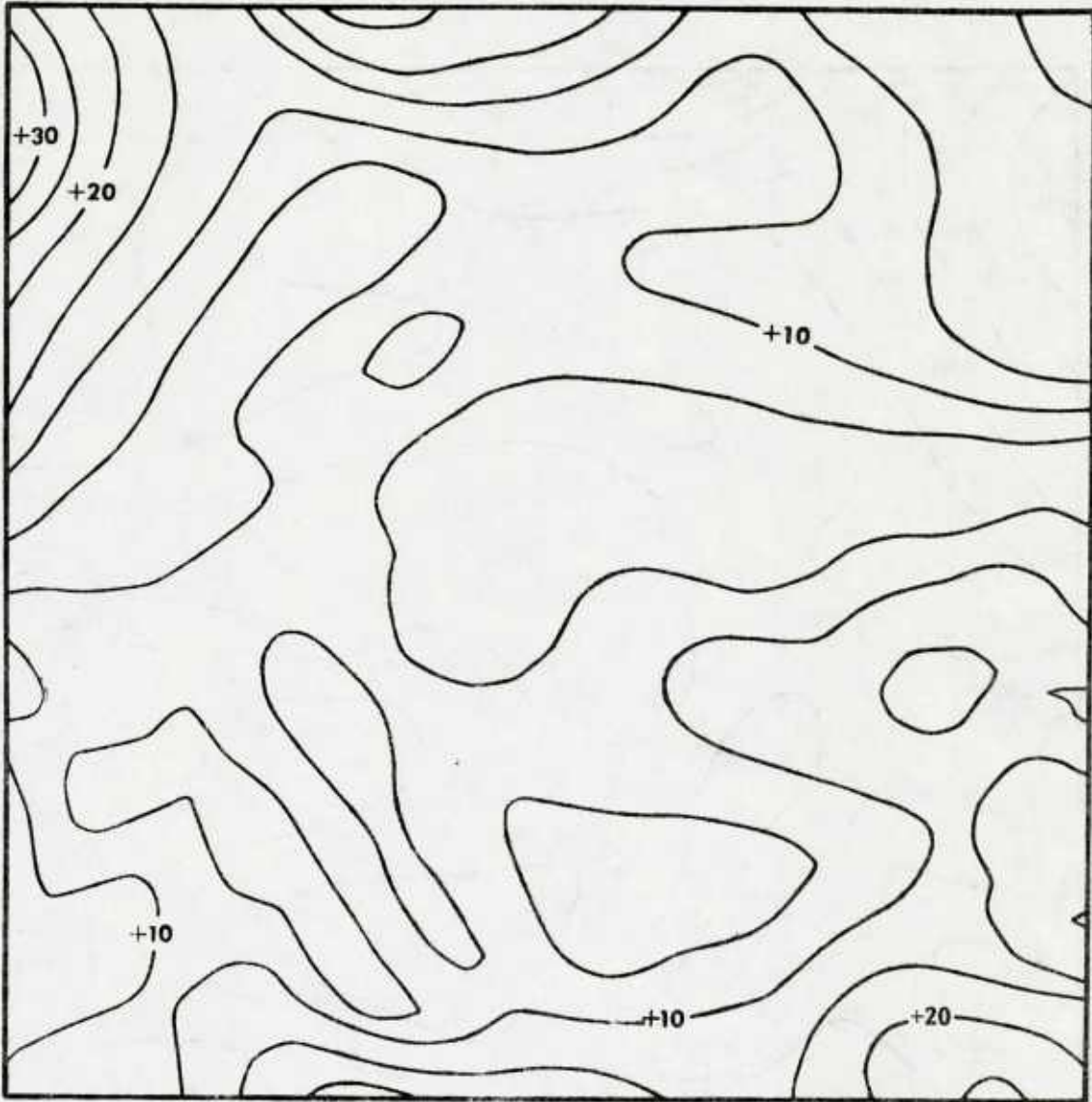


Figure 25. NVA isotachs (kt) at 700 mb, weights $(\tilde{\alpha}, \tilde{\beta}) = (60, 25)$

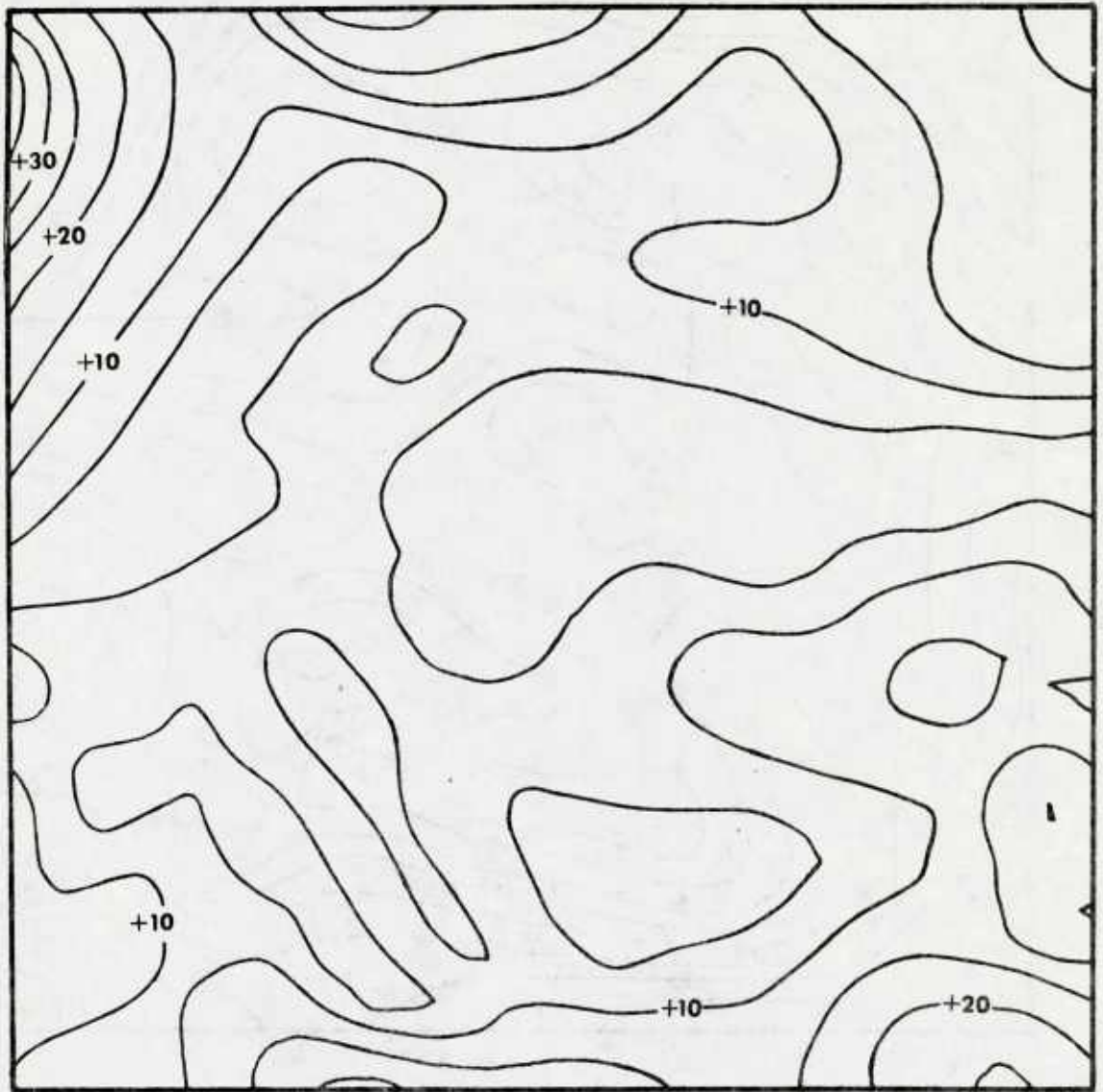


Figure 26. NVA isotachs (kt) at 700 mb, weights $(\tilde{\alpha}, \tilde{\beta}) = (55, 0)$

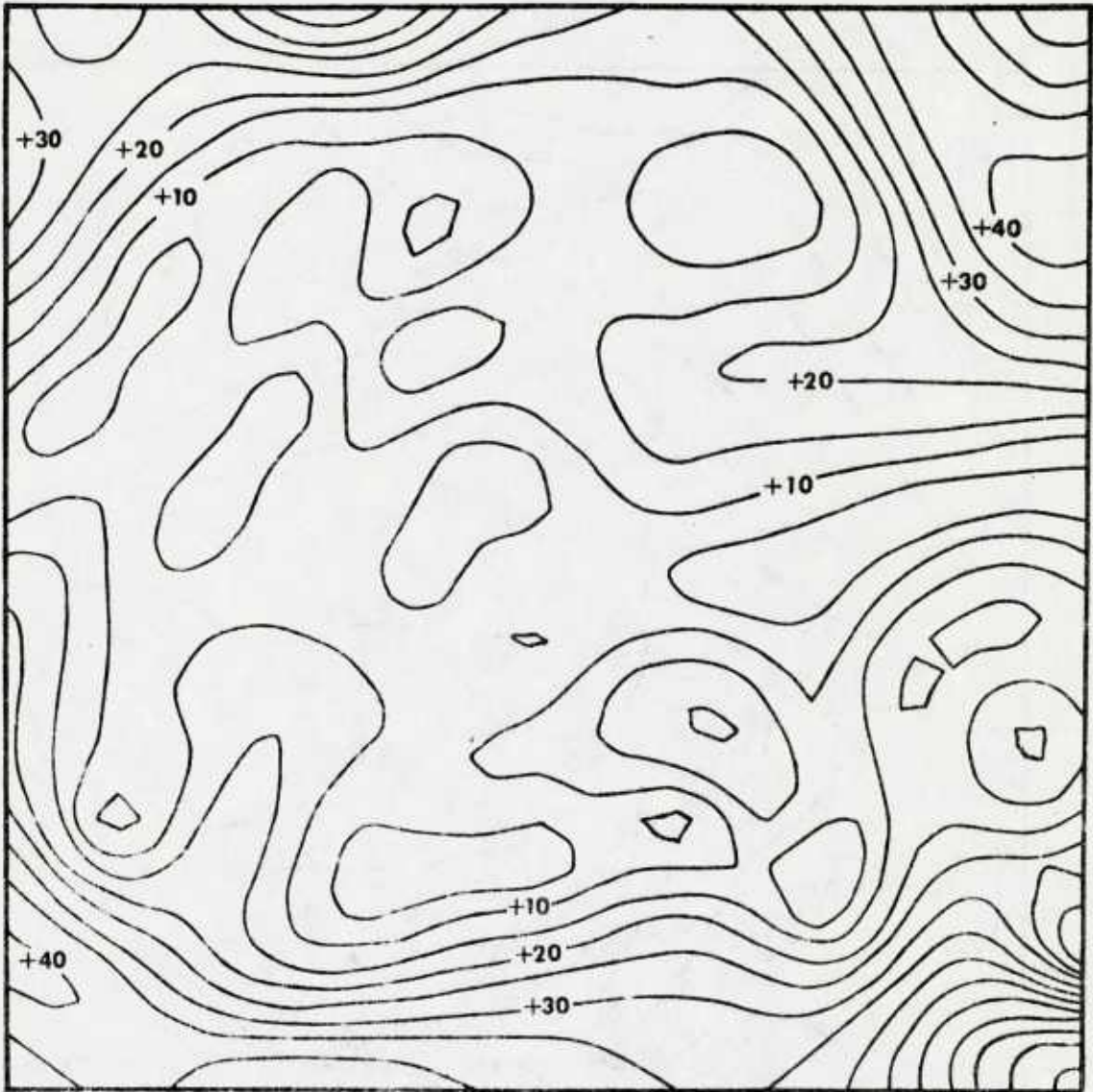


Figure 27. Initial guess isotachs (kt) at 400 mb

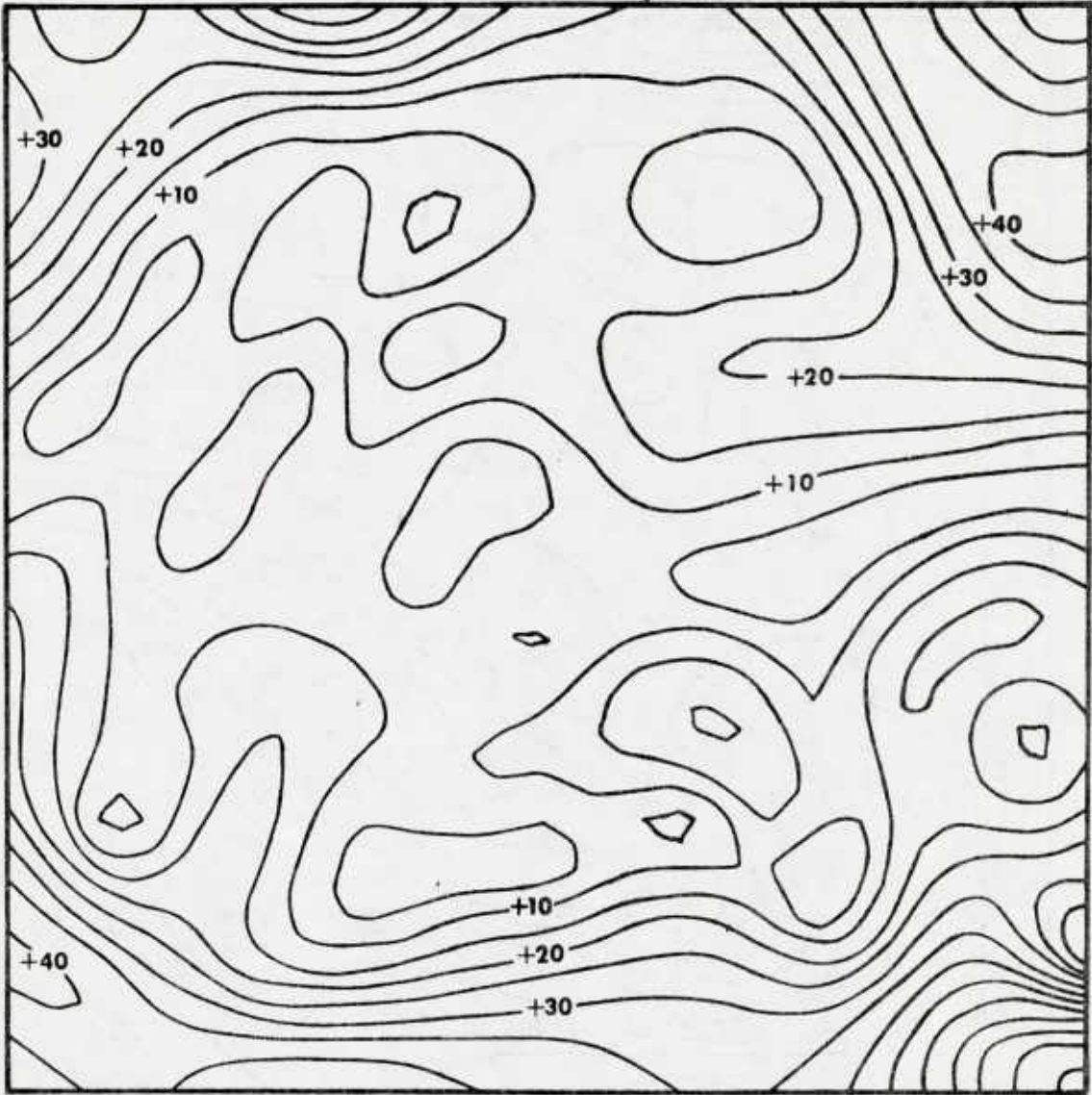


Figure 28. NVA isotachs (kt) at 400 mb, weights $(\tilde{\alpha}, \tilde{\beta}) = (60, 25)$

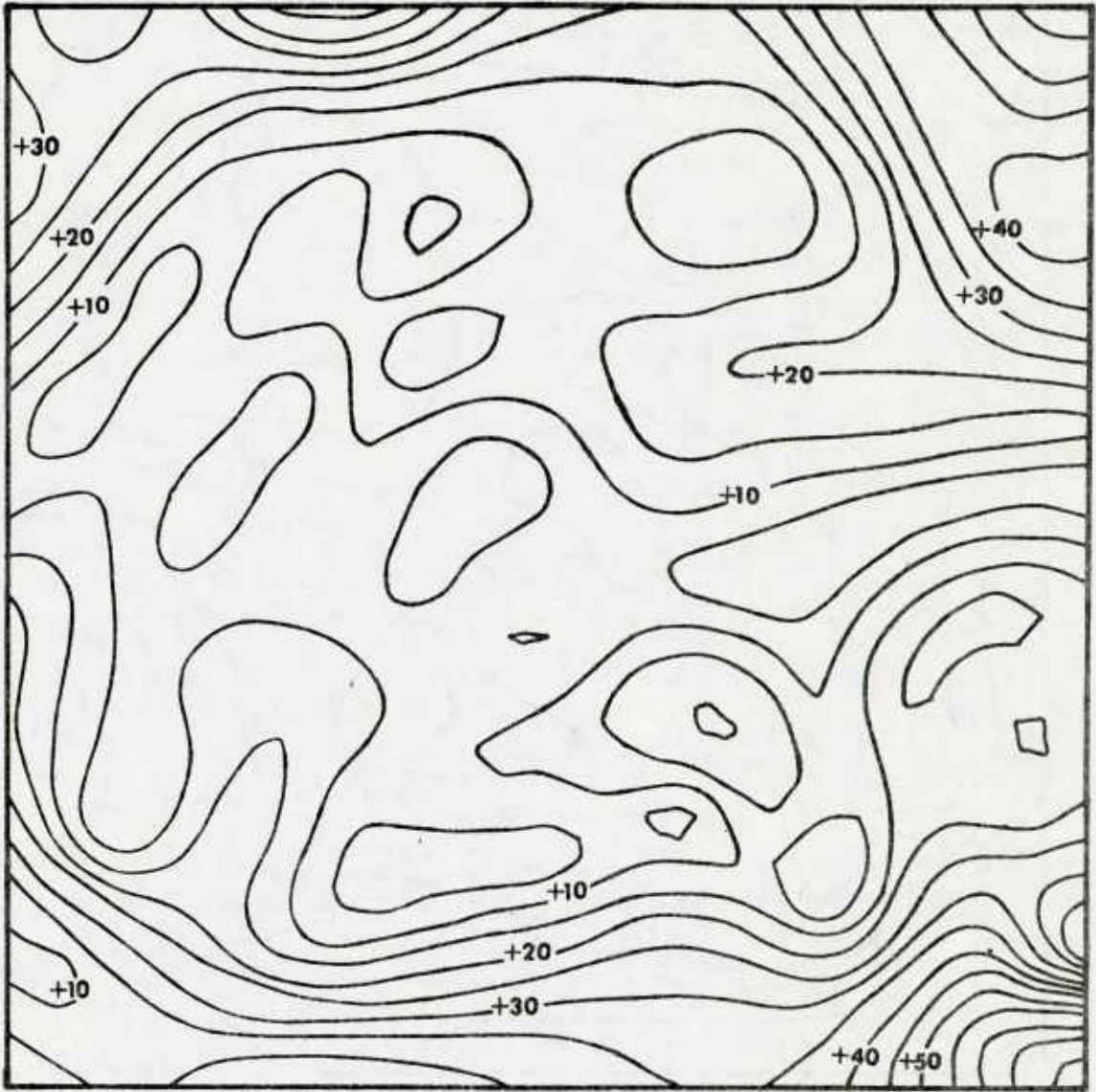


Figure 29. NVA isotachs (kt) at 400 mb, weights $(\tilde{\alpha}, \tilde{\beta}) = (55, 0)$

4. SOME ASPECTS OF THE SPECTRAL ANALYSIS OF INITIAL GUESS AND NVA FIELDS

Any technique for analysis of meteorological data has to eliminate certain undesirable quantities from the raw data. Most of the time, with the techniques in use, this is achieved by applying a low pass filter to the raw data fields. If the analysis is to be used to initiate a forecast model, this technique successfully prevents any major gravity waves from building up during solution of the forecast equations.

In use of the variational analysis technique, there is the possibility that the technique in itself provides a low pass filter due to the physical constraint forced on the data.

In order to investigate this, a two-dimensional Fourier analysis was made from the NV analysis and its initial guess. After squaring the Fourier coefficients, the ratios between the coefficients for the NVA and the coefficients for the initial guess were calculated; this means that if the outgoing number was less than 1, the energy -- with respect to that particular combination of wave numbers in x and y direction -- was reduced in the NV analysis compared to the initial guess. Results for the 925 mb temperature and wind fields are shown in Table 2 for $(\tilde{\alpha}, \tilde{\beta}) = (65, 25)$ and in Table 3 for $(\tilde{\alpha}, \tilde{\beta}) = (55, 0)$ respectively.

In the given example it does not look as if the technique in connection with the used physical constraint acts like a "filter" for any specific wavelengths. The only obvious conclusion that can be reached comparing Table 2 with Table 3 is that regardless of the weights $\tilde{\alpha}$, $\tilde{\beta}$, corrections from the initial guess are applied to approximately the same wavelengths and the smaller the weights are, the more pronounced are the corrections; i.e., if the "energy" is reduced with respect to a certain wave number, it will be reduced even more with smaller weights $\tilde{\alpha}$, $\tilde{\beta}$ and vice versa.

Table 2. Ratio between squared Fourier coefficients for NVA over coefficients for initial guess for weights $(\alpha, \beta) = (65, 25)$.

X \ Y	Wave Number y Direction												
	1	2	3	4	5	6	7	8	9	10	11	12	
TEMPERATURE Wave Number x-Direction	1	1.5	1.4	1.0	.8	.8	.8	1.0	1.1	1.1	1.1	1.0	1.0
	2	1.5	1.3	1.0	.8	.7	.9	1.0	1.2	1.3	1.2	1.2	1.1
	3	1.4	1.1	.8	.8	.8	1.1	1.3	1.4	1.4	1.5	1.4	1.3
	4	1.4	1.1	.9	.8	1.0	1.4	1.7	1.5	1.4	1.4	1.5	1.5
	5	1.4	1.2	1.0	1.0	1.2	1.7	1.8	1.5	1.2	1.1	1.3	1.6
	6	1.4	1.4	1.3	1.1	1.3	1.7	1.7	1.3	1.0	.9	1.0	1.6
	7	1.4	1.6	1.5	1.2	1.2	1.5	1.4	1.0	.8	.7	.9	1.5
	8	1.4	1.6	1.6	1.3	1.2	1.2	1.1	.9	.8	.7	.9	1.3
	9	1.3	1.5	1.5	1.3	1.1	1.0	.9	.8	.8	.8	1.0	1.1
	10	1.1	1.3	1.4	1.2	1.0	.9	.8	.7	.7	.9	1.0	1.0
	11	1.0	1.2	1.3	1.2	1.0	.8	.7	.6	.7	.8	.9	1.0
	12	.9	1.1	1.2	1.2	.9	.7	.6	.6	.6	.7	.9	1.1
U-COMPONENT Wave Number x-Direction	1	.8	.8	.8	1.0	1.2	1.4	1.5	1.7	3.6	1.3	1.5	1.4
	2	.8	.7	.8	1.1	1.4	1.5	1.7	2.2	.5	1.1	1.2	1.3
	3	.7	.7	.8	1.3	1.7	1.9	2.1	6.7	.8	1.0	1.1	1.2
	4	.9	.7	.5	11.3	19.6	*	.8	.8	1.0	1.0	1.0	1.1
	5	1.1	.9	1.5	1.0	.7	.6	.7	1.0	1.1	1.0	1.0	.9
	6	1.2	1.2	1.3	1.0	.9	.8	.9	1.0	1.1	1.1	1.0	.7
	7	1.2	1.2	1.6	1.0	.9	1.0	1.0	1.1	1.1	1.2	.6	2.1
	8	1.1	1.1	1.0	1.0	1.0	1.1	1.1	1.0	1.0	.9	3.0	1.4
	9	.9	1.0	1.3	.4	1.2	1.2	1.1	1.0	.8	.5	6.3	1.8
	10	.7	.9	1.4	.1	1.2	1.2	1.2	1.0	.8	.6	.5	.6
	11	2.4	.5	2.0	.7	1.1	1.2	1.2	1.3	1.5	1.1	.8	.7
	12	1.6	1.8	1.1	1.0	1.1	1.1	1.2	1.5	2.3	1.3	.8	.7
V-COMPONENT Wave Number x-Direction	1	.3	**	2.8	1.3	.8	.6	.8	1.0	1.2	1.2	1.2	1.2
	2	.9	1.5	1.0	.8	.8	.9	1.0	1.2	1.2	1.2	1.1	1.1
	3	1.2	1.7	.3	.7	.8	1.0	1.1	1.2	1.2	1.1	1.0	1.0
	4	1.3	1.4	1.7	2.8	.8	1.0	1.1	1.1	1.1	1.1	1.0	1.0
	5	1.4	1.5	1.5	1.7	.5	.9	1.0	1.1	1.1	1.1	1.1	1.0
	6	1.0	1.2	1.2	1.1	1.0	.9	1.0	1.0	1.1	1.1	1.1	.9
	7	3.2	18.7	.4	.8	.9	.9	.9	1.0	1.0	.9	.9	.7
	8	1.6	1.9	4.7	.6	1.0	.8	1.2	1.0	.9	.8	.7	.8
	9	1.1	1.2	1.3	1.5	1.5	1.4	1.4	1.3	1.1	.9	1.0	1.1
	10	.6	.9	1.0	1.3	1.4	1.4	1.5	8.2	.5	.4	.0	1.8
	11	.4	.7	.9	1.1	1.2	1.2	1.2	1.5	.3	.2	2.0	1.6
	12	.2	.7	.9	1.0	1.1	1.1	1.0	1.0	.9	.9	.9	.9

* 128.6

** 456326.2

Table 3. Ratio between squared Fourier coefficients for the NVA over coefficients for initial guess for weights $(\alpha, \beta) = (55, 0)$

X \ Y	Wave Number y Direction												
	1	2	3	4	5	6	7	8	9	10	11	12	
TEMPERATURE Wave Number x-Direction	1	1.6	1.5	1.1	.9	.8	.9	1.0	1.2	1.2	1.2	1.1	1.1
	2	1.8	1.6	1.0	.8	.8	1.0	1.2	1.4	1.5	1.5	1.5	1.4
	3	1.6	1.3	.9	.8	.9	1.3	1.6	1.8	1.9	1.9	1.9	1.7
	4	1.7	1.4	1.0	1.0	1.1	1.9	2.2	2.2	2.0	2.1	2.1	2.2
	5	1.7	1.6	1.2	1.3	1.4	2.3	2.5	2.0	1.6	1.5	1.7	2.3
	6	1.8	2.0	1.6	1.6	1.6	2.3	2.2	1.6	1.2	1.1	1.3	2.2
	7	1.7	2.2	1.9	1.6	1.5	1.9	1.6	1.1	.8	.8	1.0	1.8
	8	1.7	2.2	2.0	1.6	1.3	1.4	1.1	.8	.7	.7	.9	1.4
	9	1.5	1.9	1.8	1.5	1.1	1.0	.7	.6	.6	.7	.8	1.0
	10	1.2	1.6	1.6	1.3	.9	.7	.5	.5	.5	.6	.7	.8
	11	1.0	1.3	1.3	1.2	.8	.6	.4	.4	.4	.4	.6	.7
	12	.9	1.1	1.2	1.0	.7	.4	.3	.3	.3	.3	.5	.7
U-COMPONENT Wave Number x-Direction	1	.8	.8	.8	1.1	1.3	1.4	1.5	1.7	3.8	1.4	1.5	1.4
	2	.7	.7	.8	1.2	1.4	1.6	1.7	2.4	.5	1.1	1.3	1.3
	3	.7	.6	.8	1.3	1.8	2.1	2.2	8.2	.8	1.0	1.1	1.2
	4	.9	.7	.5	22.7	29.2	*	1.2	.8	1.0	1.0	1.0	1.1
	5	1.1	1.0	1.6	.9	.7	.6	.7	1.0	1.1	1.0	1.0	.9
	6	1.3	1.3	1.3	1.0	.8	.8	.9	1.0	1.1	1.1	1.0	.7
	7	1.2	1.2	1.7	1.0	.9	.9	1.0	1.1	1.2	1.2	.7	2.1
	8	1.1	1.1	.9	1.0	1.0	1.1	1.1	1.0	1.0	.9	2.9	1.4
	9	.9	1.0	1.2	.4	1.2	1.2	1.1	1.0	.8	.5	6.6	1.9
	10	.7	.9	1.4	.1	1.2	1.2	1.2	1.0	.9	.6	.5	.6
	11	2.7	.5	2.0	.7	1.1	1.2	1.3	1.4	1.6	1.1	.8	.7
	12	1.6	1.8	1.1	1.0	1.1	1.1	1.2	1.7	2.6	1.3	.8	.7
V-COMPONENT Wave Number x-Direction	1	.3	**	2.9	1.2	.7	.5	.6	.9	1.1	1.2	1.2	1.1
	2	.9	1.3	1.0	.8	.8	.8	1.0	1.2	1.2	1.2	1.1	1.1
	3	1.3	2.0	.2	.6	.8	.9	1.1	1.2	1.2	1.1	1.0	1.0
	4	1.4	1.5	1.8	4.8	.8	1.0	1.1	1.1	1.2	1.1	1.0	1.0
	5	1.4	1.5	1.6	1.9	.5	.9	1.1	1.1	1.2	1.2	1.1	1.0
	6	1.0	1.3	1.2	1.1	1.0	.7	1.0	1.0	1.1	1.1	1.1	1.0
	7	3.5	22.1	.3	.7	.9	.8	1.7	1.0	1.0	1.0	.9	.8
	8	1.7	2.1	5.4	.5	.9	.6	1.5	1.1	1.0	.9	.8	.9
	9	1.1	1.3	1.4	1.7	1.7	1.6	1.6	1.5	1.3	1.1	1.1	1.2
	10	.7	.9	1.0	1.3	1.4	1.4	1.6	11.5	.4	.3	.0	2.1
	11	.4	.7	.9	1.1	1.2	1.2	1.3	1.7	.1	.1	3.4	1.7
	12	.1	.7	.9	1.0	1.1	1.1	1.0	1.0	1.0	1.0	1.0	1.0

* 176.9

** 463859.1

It should be noted that the initial guess fields are the routine FNWC temperature and height analyses that are most probably in reasonable agreement with the physical constraint used in this analysis scheme. So the next step was to add random noise to the initial guess. White noise with a standard deviation of 1°C and 2 knots has been added to the initial guess temperature and u- and v-component fields, respectively.

Table 4 shows the ratio between the squared Fourier coefficients for the initial guess fields plus random noise over the squared coefficients for the initial guess itself. Table 5 shows the same values, calculated from the NV analysis initialized with fields plus random noise and without random noise.

If the numbers in Table 5 were equal to 1, it would mean that the NV analysis had filtered the initially added random noise completely. This is nearly valid for the temperature field and it can easily be seen that a considerable amount of the originally added noise is taken from u and v component fields after application of the NVA technique.

Table 4. Ratio between squared Fourier coefficients for initial guess plus random noise and coefficients for initial guess without random noise.

Y	Wave Number y Direction																								
	X	1	2	3	4	5	6	7	8	9	10	11	12												
TEMPERATURE	Wave Number x-Direction	1	1.1	1.0	.9	1.1	.9	1.0	1.0	1.0	1.0	1.0	1.0	1.0	1.0	1.0	1.0	1.0	1.0	1.0	1.0	1.0	1.0		
	2	1.1	1.0	.9	1.0	1.0	.9	1.0	1.1	1.0	1.0	1.1	1.1	1.0	1.0	1.1	1.0	1.0	1.0	1.0	1.0	1.0	1.0		
	3	1.0	.9	1.1	1.0	1.0	.9	1.0	1.0	1.1	1.1	1.1	1.1	1.1	1.1	1.1	1.1	1.1	1.1	1.1	1.1	1.1	1.1	1.1	
	4	.9	1.0	.9	1.1	1.0	1.0	1.1	.9	1.0	1.1	.9	1.0	1.1	1.1	1.1	1.1	1.1	1.1	1.1	1.1	1.1	1.1	1.1	
	5	1.0	1.1	1.0	1.0	1.0	1.0	1.1	1.1	1.1	1.1	1.0	1.1	1.1	1.1	1.1	1.1	1.1	1.1	1.1	1.1	1.1	1.1	1.2	
	6	1.2	.9	.9	1.0	1.1	.9	.8	1.0	1.1	1.1	1.0	1.1	1.1	1.1	1.1	1.1	1.1	1.1	1.1	1.1	1.1	1.1	1.2	
	7	.9	1.2	1.0	1.0	1.0	.9	.8	.9	.9	1.0	1.1	1.0	1.0	1.1	1.0	1.0	1.1	1.0	1.0	1.0	1.0	1.0	.9	
	8	1.0	1.1	1.1	.9	1.1	1.1	1.1	1.0	1.1	1.1	1.1	1.1	1.1	1.1	1.1	1.1	1.1	1.1	1.1	1.1	1.1	1.1	1.1	1.1
	9	.9	1.1	1.1	1.0	1.0	.9	.9	1.0	1.1	1.0	1.0	1.0	1.0	1.0	1.0	1.0	1.0	1.0	1.0	1.0	1.0	1.0	1.0	1.0
	10	.9	1.1	1.0	1.1	1.0	1.1	1.1	1.0	1.0	1.0	1.0	1.0	1.0	1.0	1.0	1.0	1.0	1.0	1.0	1.0	1.0	1.0	1.0	.9
	11	1.1	1.1	.9	1.1	1.0	.9	.9	1.0	1.0	1.0	1.1	1.1	1.1	1.1	1.1	1.1	1.1	1.1	1.1	1.1	1.1	1.1	1.1	.9
	12	.9	1.0	1.0	1.1	1.0	1.1	.9	1.1	1.1	.9	.9	1.0	1.0	1.0	1.0	1.0	1.0	1.0	1.0	1.0	1.0	1.0	1.0	.9
U-COMPONENT	Wave Number x-Direction	1	.8	.7	.6	1.3	1.0	.9	1.0	1.4	.1	1.0	1.2	1.1	1.0	1.2	1.1	1.0	1.2	1.1	1.0	1.2	1.1	1.1	
	2	.7	1.3	1.1	1.0	1.2	1.3	.9	.6	2.0	.8	1.0	1.2	1.1	.8	1.0	1.2	.8	1.0	1.2	.8	1.0	1.2	1.1	
	3	.7	1.6	.6	.5	.8	.5	2.0	5.7	1.4	1.2	.8	1.1	1.0	1.2	.8	1.1	1.0	1.2	1.1	1.0	1.2	1.1	1.1	
	4	1.4	1.8	.9	71.7	23.8	32.6	3.9	.3	1.0	1.2	.8	1.1	1.0	1.2	.8	1.1	1.0	1.2	1.1	1.0	1.2	1.1	1.1	1.1
	5	.8	.9	2.9	1.1	.6	1.2	1.5	.5	.9	.8	.8	1.0	1.1	.8	.8	.7	1.0	.8	1.1	1.0	.8	1.1	1.1	.7
	6	.8	.8	2.2	1.3	1.1	1.4	.7	1.4	1.6	1.4	1.8	1.1	1.0	1.4	1.8	3.3	1.0	1.4	1.8	3.3	1.4	1.8	3.3	3.3
	7	.9	.7	3.2	.5	.8	.8	.9	.8	.8	1.7	.0	4.5	1.0	1.7	.0	4.5	1.0	1.7	.0	4.5	1.7	.0	4.5	4.5
	8	1.1	1.0	.5	1.4	.9	.9	1.1	1.2	1.0	.4	.0	3.5	1.0	1.1	1.0	3.5	1.0	1.1	1.0	3.5	1.1	1.0	3.5	3.5
	9	.8	1.1	.8	3.1	.9	.8	1.0	.8	.7	.2	11.3	1.0	1.0	.2	11.3	1.0	1.0	.2	11.3	1.0	.2	11.3	1.0	1.0
	10	1.7	.7	.7	.3	.7	.9	.9	1.2	.9	1.0	.9	.2	1.0	1.0	.9	.2	1.0	1.0	.9	.2	1.0	.9	.2	.2
	11	.0	3.2	.4	.5	.9	.8	1.2	1.2	2.0	.3	.8	1.0	1.0	.3	.8	1.0	1.0	.3	.8	1.0	.3	.8	1.0	1.0
	12	1.9	.6	2.6	.5	.7	1.6	1.4	.3	1.4	.5	1.2	1.0	1.0	.5	1.2	1.3	1.0	.5	1.2	1.3	.5	1.2	1.3	1.3
V-COMPONENT	Wave Number x-Direction	1	7.4	*	6.9	.0	.4	.1	.9	1.8	1.3	.9	1.2	1.0	1.2	1.1	1.0	.9	1.2	1.1	1.0	1.2	1.1	1.0	
	2	.4	.2	.7	1.3	.6	.7	1.2	.9	.9	.9	1.0	1.1	1.0	.9	.9	1.0	.9	1.2	1.1	1.0	1.2	1.1	1.0	
	3	1.6	4.8	3.2	.3	1.4	.9	.9	1.0	1.0	1.0	1.0	1.0	1.0	1.0	1.0	1.0	1.0	1.0	1.0	1.0	1.0	1.0	1.0	1.2
	4	1.1	1.4	1.8	11.9	.9	.9	1.2	1.1	1.1	1.1	1.1	1.1	1.1	1.1	1.1	1.1	1.1	1.1	1.1	1.1	1.1	1.1	1.1	.8
	5	1.2	.8	.8	1.9	.7	1.3	.8	1.0	1.0	1.0	1.0	1.0	1.0	1.0	1.0	1.0	1.0	1.0	1.0	1.0	1.0	1.0	1.0	.7
	6	.6	.2	.4	1.2	1.1	3.4	1.1	1.5	.9	.8	1.6	1.0	1.0	.8	1.6	2.1	1.0	.8	1.6	2.1	.8	1.6	2.1	2.1
	7	2.0	8.8	3.9	.3	1.2	.6	10.0	.5	1.3	.7	.8	1.0	1.0	.7	.8	1.3	1.0	.7	.8	1.3	.7	.8	1.3	1.3
	8	.4	1.3	4.3	1.0	.2	.0	.3	1.8	.8	.7	1.3	1.0	1.0	.7	1.3	1.3	1.0	.7	1.3	1.3	.7	1.3	1.3	1.3
	9	.7	.8	1.7	.9	.5	2.1	.8	.6	1.5	.2	.6	1.0	1.0	.2	.6	1.6	1.0	.2	.6	1.6	.2	.6	1.6	1.6
	10	1.7	1.2	1.2	1.1	1.3	.8	1.5	3.6	1.4	1.4	2.8	1.0	1.0	1.4	2.8	1.6	1.0	1.4	2.8	1.6	1.4	2.8	1.6	1.6
	11	1.6	.7	1.2	.9	.8	.7	.8	2.1	.9	2.0	6.7	1.0	1.0	2.0	6.7	.2	1.0	2.0	6.7	.2	2.0	6.7	.2	.2
	12	.4	1.6	.7	.8	.9	1.4	1.0	1.2	1.2	.8	.5	1.0	1.0	.8	.5	1.6	1.0	.8	.5	1.6	.8	.5	1.6	1.6

* 412099.8

Table 5. Ratio between squared Fourier coefficients for NVA initialized by fields plus random noise over coefficients for NVA initialized by same fields without random noise.

X \ Y	Wave Number y Direction												
	1	2	3	4	5	6	7	8	9	10	11	12	
TEMPERATURE	Wave Number x-Direction	1	2	3	4	5	6	7	8	9	10	11	12
	1	1.0	1.0	1.0	1.0	1.0	1.0	1.0	1.0	1.0	1.0	1.0	1.0
	2	1.0	1.0	1.0	1.0	1.0	1.0	1.0	1.0	1.0	1.0	1.0	1.0
	3	1.0	1.0	1.0	1.0	1.0	1.0	1.0	1.0	1.0	1.0	1.0	1.0
	4	1.0	1.0	1.0	1.0	1.0	1.0	1.0	1.0	1.0	1.0	1.0	1.0
	5	1.0	1.0	1.0	1.0	1.1	1.0	1.1	1.0	1.0	1.0	1.1	1.0
	6	1.1	1.0	1.0	1.0	1.0	1.0	1.0	1.0	1.1	1.0	1.0	.9
	7	1.0	1.0	1.0	1.0	1.0	.9	1.0	1.0	1.0	1.0	1.0	1.0
	8	1.0	1.0	1.0	1.0	1.0	1.0	1.0	1.0	1.0	1.0	1.0	1.0
	9	1.0	1.0	1.0	1.0	1.0	1.0	1.0	1.0	1.0	1.0	1.1	1.0
	10	1.0	1.1	1.0	1.1	1.0	1.1	1.0	1.1	1.0	1.0	1.0	1.0
	11	1.0	1.1	1.0	1.0	1.0	1.0	1.0	1.0	1.0	1.0	1.0	1.0
12	1.0	1.0	1.1	1.0	1.0	1.0	1.0	1.0	1.0	1.0	1.0	1.0	
U-COMPONENT	Wave Number x-Direction	1	2	3	4	5	6	7	8	9	10	11	12
	1	.8	.8	.7	1.2	1.1	.9	1.0	1.2	.3	1.1	1.1	1.1
	2	.8	1.3	1.1	1.1	1.1	1.1	1.0	.8	2.7	.8	1.0	1.1
	3	.8	1.5	.7	.6	.9	.7	1.4	2.8	1.3	1.2	.9	1.1
	4	1.3	1.6	1.6	5.1	4.0	2.5	.0	.5	1.0	1.1	.9	1.1
	5	.9	1.1	2.2	1.0	.6	1.3	1.5	.7	.9	.9	.9	.8
	6	.8	.7	1.7	1.3	1.1	1.3	.8	1.2	1.3	1.4	1.6	3.1
	7	.9	.8	2.2	.6	.9	.9	.9	.9	.9	1.5	.0	2.1
	8	1.0	.9	.9	1.2	1.0	.9	1.1	1.1	1.0	.4	.6	1.9
	9	.8	1.0	.9	2.2	.9	.8	1.0	.9	.8	.2	2.7	1.0
	10	1.5	.9	.8	1.3	.8	.9	.9	1.1	.9	1.0	1.1	.3
	11	1.5	2.9	.4	.7	.9	.9	1.1	1.1	1.3	.5	.9	1.0
12	1.5	.7	1.7	.8	.8	1.3	1.3	.7	1.2	.9	1.2	1.2	
V-COMPONENT	Wave Number x-Direction	1	2	3	4	5	6	7	8	9	10	11	12
	1	14.6	3.1	2.9	.1	.6	.2	1.0	1.5	1.2	.9	1.1	1.0
	2	.5	.0	.6	1.2	.7	.8	1.2	1.0	.9	.9	1.0	1.0
	3	1.5	3.0	5.1	.4	1.4	.9	.9	1.0	1.0	1.0	1.0	1.1
	4	1.1	1.2	1.4	11.2	.9	1.0	1.1	1.0	1.1	1.1	1.2	.8
	5	1.0	.9	.8	1.4	1.0	1.2	.9	.9	1.0	1.1	.8	.8
	6	.6	.4	.7	1.1	1.2	3.9	.9	1.3	.9	.9	1.4	1.7
	7	1.4	2.5	3.3	.4	1.1	.7	7.1	.7	1.2	.9	.8	1.3
	8	.8	1.2	1.4	1.1	.3	.0	.7	1.6	.8	.8	1.3	1.4
	9	.8	.8	1.3	1.1	.9	1.7	.8	.9	1.2	.4	.8	1.4
	10	1.5	1.2	1.2	1.0	1.1	.9	1.2	1.7	1.4	1.2	34.8	1.3
	11	1.7	.8	1.1	.9	.8	.8	.9	1.3	1.6	1.9	.3	.5
12	.0	1.4	.8	.8	1.0	1.3	1.0	1.2	1.2	1.0	.7	1.3	

5. CONCLUSIONS

It has been shown that the NVA technique with the given physical constraint leads to reasonable results. Relatively small random noise on the initial guess is properly smoothed. However, before running the analysis routinely, a forecast model has to be initialized in order to find the best set of weights on the initial guess data. The incorporation of the data assembling process into the scheme should be considered because it might prove that otherwise the method is too time consuming if assembling and analyzing are two separate computational processes.

REFERENCES

- Kesel, P. and H. Lewit, 1973: Application of existing NVA surface and upper-air analysis models to the EPRF MED window. ODSI, Task 4 report prepared under Contract W66314-73-C-1591.
- Lewis, J., 1972: An operational upper-air analysis using the variational method. Tellus, 24, No. 6, 514-530.
- Sasaki, Y., 1970a: Some basic formalisms in numerical variational analysis. Mon. Wea. Rev., 98, No. 12, 875-883.
- Sasaki, Y., 1970b: Numerical variational analysis formulated under the constraints as determined by longwave equations and a low-pass filter. Mon. Wea. Rev., 98, No. 12, 884-898.
- Sasaki, Y., 1970c: Numerical variational analysis with weak constraint and application to surface analysis of severe storm gust. Mon. Wea. Rev., 98, No. 12, 899-910.

DUDLEY KNOX LIBRARY - RESEARCH REPORTS



5 6853 01078714 6

U168561